NeuroImage 202 (2019) 116116

Contents lists available at ScienceDirect

NeuroImage

journal homepage: www.elsevier.com/locate/neuroimage

Sex-related differences in intrinsic brain dynamism and their neurocognitive correlates

Nina de Lacy [a,*], Elizabeth McCauley [a], J. Nathan Kutz [b], Vince D. Calhoun [c]

[a] Department of Psychiatry and Behavioral Sciences, University of Washington, 1959 NE Pacific St, Seattle, WA, 98195, USA
[b] Department of Applied Mathematics, University of Washington, Lewis Hall 201, Seattle, WA, 98195, USA
[c] Tri-institutional Center for Translational Research in Neuroimaging and Data Science (TReNDS) [Georgia State University, Georgia Institute of Technology, Emory University], Atlanta, GA, 30303, USA

ARTICLE INFO

Keywords:
Intrinsic networks
ICA
Sex-related
Dimorphism
Functional MRI
Dynamic functional connectivity
Dynamism

ABSTRACT

The application of dynamic or time-varying connectivity techniques to neuroimaging data represents a new and complementary method to traditional static (time-averaged) methods, capturing additional patterns of variation in human brain function. Dynamic connectivity and related measures of brain dynamism have been detailed in neurotypical brain function, during human development and across neuropsychiatric disorders, and linked to cognitive control and executive function abilities. Despite this large and growing body of work, little is known about whether sex-related differences are present in dynamic connectivity and brain dynamism, a question pertinent to our understanding of brain function in both health and disease, given the sex bias observed in the prevalence of neuropsychiatric disorders, and well-demonstrated sex-related differences in the performance of certain neurocognitive tasks. We present the first analyses of sex-related effects in dynamic connectivity and brain dynamism referenced to neurocognitive function, in a large sample of sex-, age- and motion-matched subjects in 24- and 51-network whole brain functional parcellations. We demonstrate that sexual dimorphism is present in human dynamic connectivity and in multiple high-order measures of brain dynamism, as well as validating prior work that sex-related differences exist in static intrinsic connectivity. We also provide the first evidence suggesting a link between differential neurocognitive performance by males and females and brain functional dynamics. Reduced dynamism in females, who spend more time in certain brain states and switch states less frequently, may provide a 'stickier' functional substrate associated with slower response inhibition, whereas males exhibit greater dynamic fluidity, change between certain states more often and range over a larger state space, achieving superior performance in mental rotation, which demands an iterative visualization and problem-solving approach. We conclude that sex is an important variable to consider in functional MRI experiments and the analysis of dynamic connectivity and brain dynamism.

1. Introduction

The question of whether males and females display differences in their neurocognitive processing abilities, brain structure and function, has long been of interest in human neuroscience research. A large body of work in psychology has described significant sex-related differences in the performance of neurocognitive tasks. Earlier research found widespread differences in various cognitive abilities. More recently, additional studies have confirmed differences in a somewhat narrower array of tasks. Perhaps the most commonly replicated findings are that males appear to exhibit consistently superior performance in certain visuospatial tasks, and may be represented at above-average rates among high performers in mathematics, while females perform better at reading and certain tasks of verbal fluency, episodic and recognition memory (D. I. Miller and Halpern, 2014). These differences can be quite specific and circumscribed. For example, males perform better in tasks of mental rotation, though the difference between males and females is wider for 3-dimensional versus 2-dimensional objects (Voyer et al., 1995). It is recognized that the formation of sex-related cognitive differences may be complex in origin, with environmental and/or sociocultural influences contributing to performance differentials. Further, considerable variation exists at the level of the individual. However, in certain tasks such as reading the differences between male and female performance appear considerable, even when educational and cultural factors are accounted

* Corresponding author.
E-mail address: delacyn@uw.edu (N. de Lacy).

https://doi.org/10.1016/j.neuroimage.2019.116116
Received 16 July 2019; Accepted 20 August 2019
Available online 22 August 2019

for and large sample sizes are surveyed (Stoet and Geary, 2013).

Concomitantly, the quantification of neuroanatomical dimorphism, and exploration of potential neural correlates of the sex-related differences observed in cognition, have also attracted substantial research interest. The earliest generation of macroscale studies in humans focused on volumetric analyses using structural magnetic resonance imaging (MRI). These identified not only a menu of brain regions with significant differences in volume between sexes, but also suggested regional growth trajectories may vary between boys and girls (De Bellis et al., 2001; Lenroot and Giedd, 2008; Lenroot et al., 2007; Raznahan et al., 2010). Recent studies have continued to support volumetric and white-matter differences between males and females as being region-specific (Guadalupe et al., 2017; Sacher et al., 2013) and further suggested that sex-related differences in cortical thickness and gyrification exist (Im et al., 2006; Mutlu et al., 2013). In addition, use of diffusion tensor techniques has identified prominent differences in the structural white-matter connectome, such as greater within-hemispheric connectivity in males and between-hemispheric connectivity in females (Ingalhalikar et al., 2014b), though these have not been undisputed (Ingalhalikar et al., 2014a; Joel and Tarrasch, 2014).

Functional MRI (fMRI) has similarly supported a body of work investigating sex-related differences in brain function, encompassing the performance of in-scanner tasks, as well as correlation of ex-scanner task performance with observations derived from task-free, or resting-state fMRI (rsfMRI). For example, sex-related differences have been identified during the performance of visuospatial tasks (Gur et al., 2000), paralleling observations derived from the psychological literature. In rsfMRI, spontaneous brain activity is recorded, with robust evidence suggesting this intrinsic activity exhibits the characteristics of a weakly-correlated system with considerable spatio-temporal organization. Many studies have identified sets of macroscale *intrinsic networks* in rsfMRI and explored inter-individual and group differences in their function. Individual intrinsic networks appear to have specific functional associations (Laird et al., 2011) and resemble networks observed during task performance (Smith et al., 2009). Analyses quantifying the relative strength of statistical correlations among brain regions within these intrinsic networks is often termed functional connectivity, with that of connections among networks deemed *functional network connectivity* (FNC).

Controversy also exists regarding the presence of sex-related differences in functional connectivity. While some studies have described sex-related differences in fronto-parietal, cingulo-opercular and temporal connections in typically-developing adults (Biswal et al., 2010; Zuo et al., 2010) and youth (Satterthwaite et al., 2015) or individual networks such as the salience and default mode network (DMN) in healthy ageing (Jamadar et al., 2018), others have found no differences between males and females in certain prominent intrinsic networks (Weissman-Fogel et al., 2010). Though fewer studies have been performed focusing on sex-related differences in FNC, these have also been identified. For example, Allen et al. examined sex-related differences in FNC in the context of a multivariate connectivity analysis in a large sample of neurotypical adults, and found that connections among many major intrinsic networks exhibited significant sex-related differences after controlling for other factors such as age (Allen et al., 2011).

Historically, connectivity analyses using rsfMRI data utilized time-averaging across the neuroimaging timecourse to identify dominant patterns of spatio-temporal connectivity, producing a 'snapshot' of functional connectivity. This has been termed *static* connectivity analysis. More recently techniques have been developed that leverage machine learning to tease out the temporal structure of spatial connections (Hutchison et al., 2013). For example, a leading approach employs a windowing and clustering strategy to estimate multiple, separable connectivity patterns within neuroimaging data (Damaraju et al., 2014). In recent years, many studies have focused on these concepts of *dynamic connectivity*, with the temporal relationship among intrinsic networks increasingly viewed through this prism of time-varying, transient brain states, among which subjects transition over time (Calhoun et al., 2014). Concomitantly, we and other groups have developed a series of secondary metrics that quantify inter-individual and group differences in brain *dynamism*, embodying concepts of fluidity, range and transitions within computational subspaces that may be derived from dynamic functional connectivity matrices (R. L. Miller et al., 2016). Early studies (Jia et al., 2014; Nomi et al., 2017; Z. Yang et al., 2014) suggest that there may be relationships between brain functional dynamism and cognitive abilities in humans. A previous study has explored sex-related differences in the occupancy of temporally independent brain states (Yaesoubi et al., 2015). However, none to our knowledge have established the extent of differences between males and females in dynamic connectivity using more standard spatial ICA, or analyzed sex-related differences in metrics of dynamism, and their relationship to the cognitive abilities that classically display sex-related differences in performance.

Despite decades of research, sex-related differences in human brain function and cognition continue to generate significant debate. Fueled by "a perfect storm of advances in the biology, changes in policy at major granting institutions, hyperbolic exaggeration by the media and strong pushback by select scientists … the subject of sex differences in the brain is singular for both its broad importance and its impact…" (McCarthy, 2016). Besides being an open question in neuroscience, this is also a compelling issue from a translational standpoint, given the pervasive sex bias in the incidence, prevalence and severity of many neuropsychiatric disorders. While sociocultural factors may influence these disparities, significant differences in the incidence of disorders with identifiable biological correlates such as autism, multiple sclerosis and certain dementias argue that sex is at a minimum a meaningful biological variable pertinent to their mechanisms. Further, the disambiguation of biological, environmental and sociocultural variables in explaining sex-related differences in neuropsychiatric disease requires the establishment of baseline dimorphism in brain structure and function. Given the large and growing number of rsfMRI studies in health and disease, this is a pressing research question.

We aimed to bring together the important and timely topic of sex-related differences in human brain function with rapidly advancing research techniques to analyze sex-related differences in dynamic functional connectivity (dFNC). We asked whether males and females display significant differences in dFNC and metrics of brain dynamism. Based on prior evidence from static functional connectivity analysis (sFNC) and brain structural work, we hypothesized that significant sex-related differences would be present in dFNC. Further, we had a tentative hypothesis that sex-related differences in brain dynamism would correlate with performance on tasks of mental rotation, given extant work in psychometric studies and the - albeit small - evidence base suggesting relationships between dynamism and cognitive performance. In this study, we analyze sex-related differences in sFNC, dFNC and dynamism metrics using two functional parcellations estimated using group spatial independent component analysis (ICA) in a large age- and gender-matched subject sample drawn from the Brain Genomics Superstruct repository. Subjects were also matched for head motion. This data was selected given its high quality (due to oversampling of young, healthy adult subjects), and because performance data are available from ex-scanner tasks of mental rotation and response inhibition. Using an established pipeline (Fig. 1), we computed the effect of sex in sFNC, 7 metrics of brain dynamism, and dFNC in 4 dynamic connectivity states in 24- and 51-network parcellations. A variety of sensitivity analyses were also performed. We also explored relationships between dynamism and performance in mental rotation and response inhibition. This study represents the first analysis of sex-related differences in spatial dFNC and brain dynamism and their intrinsic neurocognitive correlates.

2. Materials and methods

Methods used in this study are presented below in the order in which they were performed (See also: Fig. 1). In summary, after pre-processing

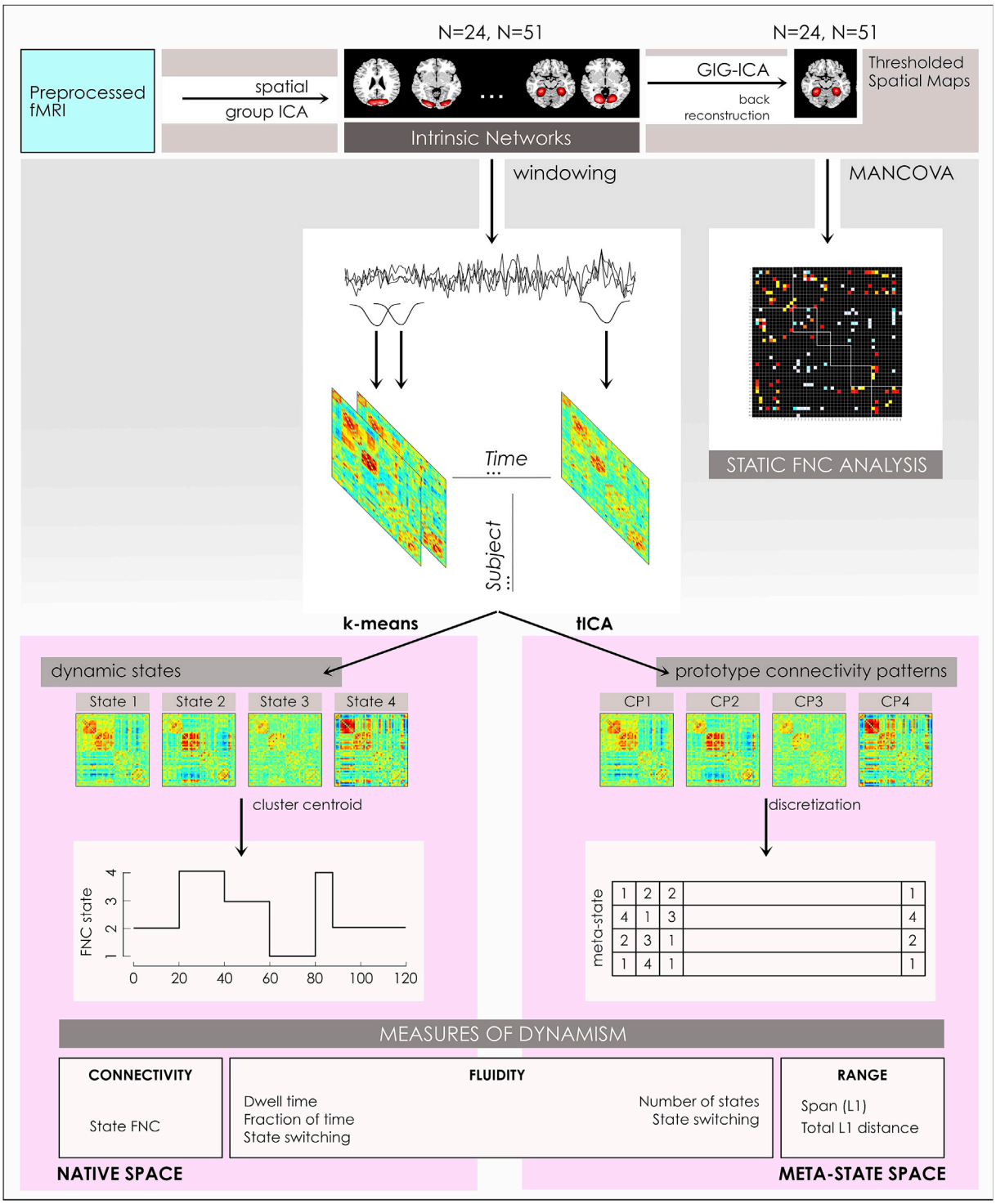

Fig. 1. Computational pipeline. A schematic of the computational pipeline illustrates steps in the preparation of the outcome measures of sFNC, dFNC and dynamism. Preprocessed fMRI were submitted to spatial group ICA to estimate 24- and 51-network models of intrinsic networks, from which thresholded spatial maps are prepared via back-reconstruction using the GIG-ICA algorithm. Pearson pairwise correlations averaged over the timecourses for these spatial maps were analyzed using a MANCOVA to form the basis for the static FNC analysis. In the dynamic pipelines, a sliding window approach to the IN timecourses formed windowed FNC that were clustered using k-means to estimate 4 brain states, on which 3 measures of dynamism were computed in the native state space. Similarly, windowed FNC were clustered using the tICA algorithm to identify prototype connectivity patterns that were discretized to form the basis for 4 measures of dynamism computed in the meta-state space.

the MRI scans using SPM12, an age-, sex- and motion-matched sample of 534 subjects was constructed and 24- and 51-network whole brain functional parcellations were estimated with group spatial ICA using GIFT. Subsequently, connectivity analysis was performed with GIFT using the component timecourses obtained from group spatial ICA to examine sex-related differences in static and dynamic network connectivity and 7 measures of brain dynamism.

2.1. Data

This study uses data from the Brain Genomics Superstruct project, collected from >3,000 individuals in the Boston community enrolled in studies of normal brain function or as controls in clinical studies (https://www.neuroinfo.org/gsp). From this larger initiative, the originators formed and released a repository in 2015 comprising demographic, MRI and behavioral data from a subset of 1570 healthy young adults ages 18–35. The originators of the data performed extensive quality control on the MRI data prior to selecting datasets for release. This included screening for "artifacts, acquisition problems, processing errors and excessive motion with each image viewed on a per-slice basis along each principal axis". 54 participants were excluded on this basis. Slice-based temporal signal-to-noise ratio (sSNR) was also computed and a further 88 participants with sSNR <100 were excluded from release (Holmes et al., 2015). Thus, every participant in the current study has an sSNR greater than 100. Age was specified within 2-year bins. For example, the 19 year-old bin includes subjects aged 18 and 19 at the time of scanning. Our study uses data from subjects in this latter sample, where the "dispersion of estimated IQ scores [was] positively shifted relative to the general population" but personality traits "have distributions that would be expected of a clinically-screen population-based sample" (Holmes et al., 2015). Of note, IQ scores were derived from Shipley-Hartford Age-Corrected T scores. Averaged individual performance data was also available for the Eriksen flanker task and a task of mental rotation. In the latter subjects completed 9 trials of 4 rotation conditions (0°, 80°, 120° and 180°) to match pairs of 3-dimensional, asymmetric groups of cubes. A modified version of the flanker was presented and subjects completed 192 trials in 8 switch and 8 non-switch blocks of 12 trials each. The present study was deemed not human subjects research by the University of Washington Institutional Review Board.

2.2. MRI pre-processing

MRI scans were collected using matched 3T TIM Trio systems at Harvard University and Massachusetts General Hospital using vendor-supplied 12-channel head coils, on 5 different scanners. 124 volumes (6.12 minutes) of functional MRI were acquired with 47 slices, interleaved sequence, voxel size 3.0 × 3.0 × 3.0 mm and TR = 3000 ms, with subjects instructed to keep their eyes open. Full details of parameters may be viewed at the Brain Genomics Superstruct website (https://static1.squarespace.com/static/5b58b6da7106992fb15f7d50/t/5b68650d8a922db3bb807a90/1533568270847/GSP_README_140630.pdf). As recommended by the originators of the data, the first 4 volumes of each scan were removed to account for scanner equilibration effects, with 120 timepoints remaining. Subsequently, we slice-time corrected remaining volumes to the middle volume, realigned to the first volume, resliced, coregistered, and normalized to the functional template and smoothed at 6 mm full width half maximum using standard algorithms in SPM12. After processing, data were submitted to quality control to assess the quality of the normalization and degree of subject motion by computing 1) spatial regression between each normalized functional image and a group mask constructed from all subjects and 2) root mean square difference of volume N to volume N+1, also known as DVARS (Christodoulou et al., 2013; Power et al., 2014). All subjects had >85% correspondence between their normalized image and the group mask with one exception. Normalization for this subject proved uncorrectable and this participant was eliminated from further consideration.

2.3. Subject sample construction

The 534-subject sample for this study was constructed by selecting right-handed subjects with estimated IQ scores available, and then sex-matching and matching for head motion (using the DVARS statistic) within age bins. There was a significant difference (2-sample *t*-test, $p < 0.05$) in IQ between males and females, with males having slightly higher mean IQ than females. In addition, there were significant differences in performance (2-sample *t*-test, $p < 0.05$) in certain neurocognitive task measures. Subject demographics and statistics related to neurocognitive task performance measures may be viewed in Table 1 and a list of subjects with their original study ID codes inspected in Supplementary Table 1. The terms 'sex', 'male' and 'female' are used in this paper in accordance with the phenotypic nomenclature used by the Brain Genomics Superstruct project.

2.4. Group spatial independent component analysis

2.4.1. Estimation of functional parcellations with group spatial independent component analysis

Group spatial independent component analysis (ICA) was performed on the pre-processed data using the Group ICA of fMRI Toolbox (GIFT) developed in our group, and widely used in ICA of fMRI (Calhoun and Adali, 2012; Calhoun et al., 2001). We performed two ICA decompositions to test the sensitivity of results to model parameters and provide an increasingly detailed view of brain networks. Resting-state scans were first pre-whitened followed by a subject-specific data reduction principal components analysis retaining 50 and 110 principle components (PCs) respectively, with the objective of stabilizing back reconstruction and retaining maximum variance at the individual level. Group ICA decompositions were then performed with 40 and 100 components respectively using the Infomax algorithm run 10 times with random initialization using ICASSO (Himberg et al., 2004; Li et al., 2007). Aggregate spatial maps were estimated as the centrotypes of component clusters to reduce sensitivity to initial algorithm parameters. Single-subject images were concatenated in time to perform the single group ICA estimation and subject specific spatial maps estimated using back reconstruction (Erhardt et al., 2011) with the group information guided ICA (GIG-ICA) algorithm (Du et al., 2016), an approach which we have shown well-captures individual subject variability (Allen et al., 2012). GIG-ICA estimates single-subject images and timecourses from the single group ICA estimation, thereby allowing individual variation in spatial maps constructed from each component (see below). The resulting independent components were scaled by converting each subject component image and the time course to z-scores.

2.4.2. Sorting components from the group spatial ICA

For each of the ICA decompositions or model orders, we sorted components into gray-matter networks versus (vs) artifactual noise components with a combination of expert visual inspection by NdL and VDC, and quantitative metrics. For each component, we computed the quantitative spectral metrics of 1) Fractional amplitude of low frequency fluctuations and 2) Dynamic range (Allen et al., 2011). The former is the ratio of the integral of spectral power below 0.10 Hz to the integral of power between 0.15 and 0.25 Hz. Dynamic range is the difference between the peak power and minimum power at frequencies to the right of the peak. Generally, components representing gray matter have higher values in these metrics, while artefactual components (such as signals accruing from cerebrospinal fluid, vascular pulsations, white matter or head motion) have lower values, though there are currently no absolute cut-off points for inclusion or exclusion. Components were inspected by NdL and VDC and those with poor overlap with cerebral gray matter or low spectral metrics were discarded. We retained 24 components from the 40-component and 51 from the 100-component ICA, each considered a set of functional intrinsic brain networks (INs).

2.4.3. Construction of intrinsic functional network spatial maps

We constructed a spatial map for each IN retained after the sorting process by selecting voxels that represented the strongest and most consistent coactivations, by performing a voxelwise one-sample *t*-test on the individual subject timecourses and thresholding individual voxels at (mean + 4 standard deviations), again following an established pipeline

Table 1
Subject demographics and neurocognitive task performance.

	Females		Males		Group Difference
	Mean	Standard Deviation	Mean	Standard Deviation	(p<0.05)
Characteristics					
Age	21.6	2.8	21.6	2.9	-
IQ	113.0	9.0	114.8	8.4	1.541E-02
DVARS	17.72	1.89	17.94	2.08	-
Absolute Displacement (mm)	0.72	0.55	0.81	0.57	-
Neurocognitive Measures					
Flank_S_CORRpc	1.0	0.0	0.9	0.0	-
Flank_S_meanRTcorr	802.7	148.7	720.4	115.7	3.330E-12
Flank_S_medRTcorr	742.1	120.9	678.3	97.9	5.891E-11
Flank_S_score	86.2	7.2	85.7	7.5	-
Flank_NS_CORRpc	1.0	0.0	1.0	0.0	1.517E-01
Flank_NS_meanRTcorr	620.5	90.6	561.3	79.6	7.856E-15
Flank_NS_medRTcorr	579.8	75.5	529.3	67.6	3.323E-15
Flank_NS_score	91.8	3.9	91.3	4.9	-
Flank_CORRpc	1.0	0.0	1.0	0.0	-
Flank_meanRTcorr	710.0	114.6	639.6	92.1	3.016E-14
Flank_medRTcorr	663.2	90.5	603.1	78.0	1.857E-15
Flank_TOT_score	178.0	9.6	177.0	10.6	-
MenRot_0_CORRpc	0.9	0.1	0.9	0.1	1.431E-02
MenRot_0_meanRTcorr	4515.1	2213.0	4862.6	2110.3	6.438E-02
MenRot_0_medRTcorr	3681.7	1807.9	3708.2	1622.6	-
MenRot_80_CORRpc	0.8	0.2	0.9	0.2	1.196E-09
MenRot_80_meanRTcorr	6438.5	3441.0	6811.5	3112.0	-
MenRot_80_medRTcorr	5892.9	3199.8	6088.1	2815.9	-
MenRot_120_CORRpc	0.7	0.2	0.8	0.2	5.514E-05
MenRot_120_meanRTcorr	6957.6	3475.5	7319.6	3420.5	-
MenRot_120_medRTcorr	6210.4	2957.8	6696.2	3289.7	-
MenRot_160_CORRpc	0.7	0.2	0.7	0.2	4.406E-06
MenRot_160_meanRTcorr	7867.4	4597.1	8645.1	4780.1	-
MenRot_160_medRTcorr	7290.8	4302.7	8000.1	4330.2	-
MenRot_TOT_CORRpc	0.8	0.1	0.8	0.1	3.080E-09
MenRot_TOT_meanRTcorr	6313.1	3072.4	6812.2	2955.6	-
MenRot_TOT_medRTcorr	5629.1	2708.2	5948.6	2435.6	-

Demographic characteristics for males and females in the 534-subject study sample. Where a significant difference was observed (2-sample *t*-test, $p < 0.05$) between males and females the statistical significance level is also displayed. Group average performance on individual measures in the Flanker task of response inhibition and a mental rotation task is similarly shown and full results may be inspected in Supplementary Table 2. Empty cells indicate insignificant results ($p > 0.05$). Expanded definitions of the labels for each neurocognitive measure may be found in Supplementary Table 3, which is a key prepared by the Brain Genomics Superstruc project.

(Allen et al., 2011) using GIFT. Thus, these spatial maps represent the brain regions most associated with each component's timecourse, instantiated in thresholded brain maps. This procedure enabled us to construct a group spatial map for each of the INs assembled from the relevant individual subject timecourses, in each of the model orders. These spatial maps were used to attribute the neurocognitive labels for each IN, and served as the inputs for the sFNC analysis to construct the sFNC matrices. Three-dimensional renderings of the resulting 3 sets of intrinsic networks may be inspected in Neurovault at https://neurovault.org/collections/4031/(24-network model) and https://neurovault.org/collections/4032/(51-network model). Each intrinsic network is labelled with its attributed neurocognitive function and number, corresponding to Fig. 2.

2.4.4. *Functional Intrinsic Network Attribution and Grouping*

The primary neurocognitive function of each IN spatial map was attributed by visual inspection and quantitative comparisons using three methods. Firstly, we determined the coordinates in Montreal Neurologic Space (MNI) associated with peak intensities for each IN in each of the 3 sets of maps. The top 3 co-ordinates were compared with the literature. We found multiple literature-based confirmatory sources that gave specific Talairach or MNI coordinates and associated these with network labels for all networks in the task-positive network group, the DMN and primary sensorimotor and visual networks, (Dosenbach et al., 2006, 2007; Fox et al., 2005; Laird et al., 2011; Seeley et al., 2007; Smith et al., 2009; Spreng et al., 2013; Vernet et al., 2014) but not for INs in the subcortical or speech/language groups. Secondly, the top 5 spatial locations in each IN were examined using the Brodmann Interactive Atlas (http://www.fmriconsulting.com/brodmann/Interact.html). Thirdly, network correlations with reverse inference maps of regional activations associated with specific neurocognitive functions were inspected in Neurosynth (Yarkoni et al., 2011). Attributions using the third method may be explored by readers by loading a spatial map in Neurovault and accessing the 'Cognitive Decoding' function.

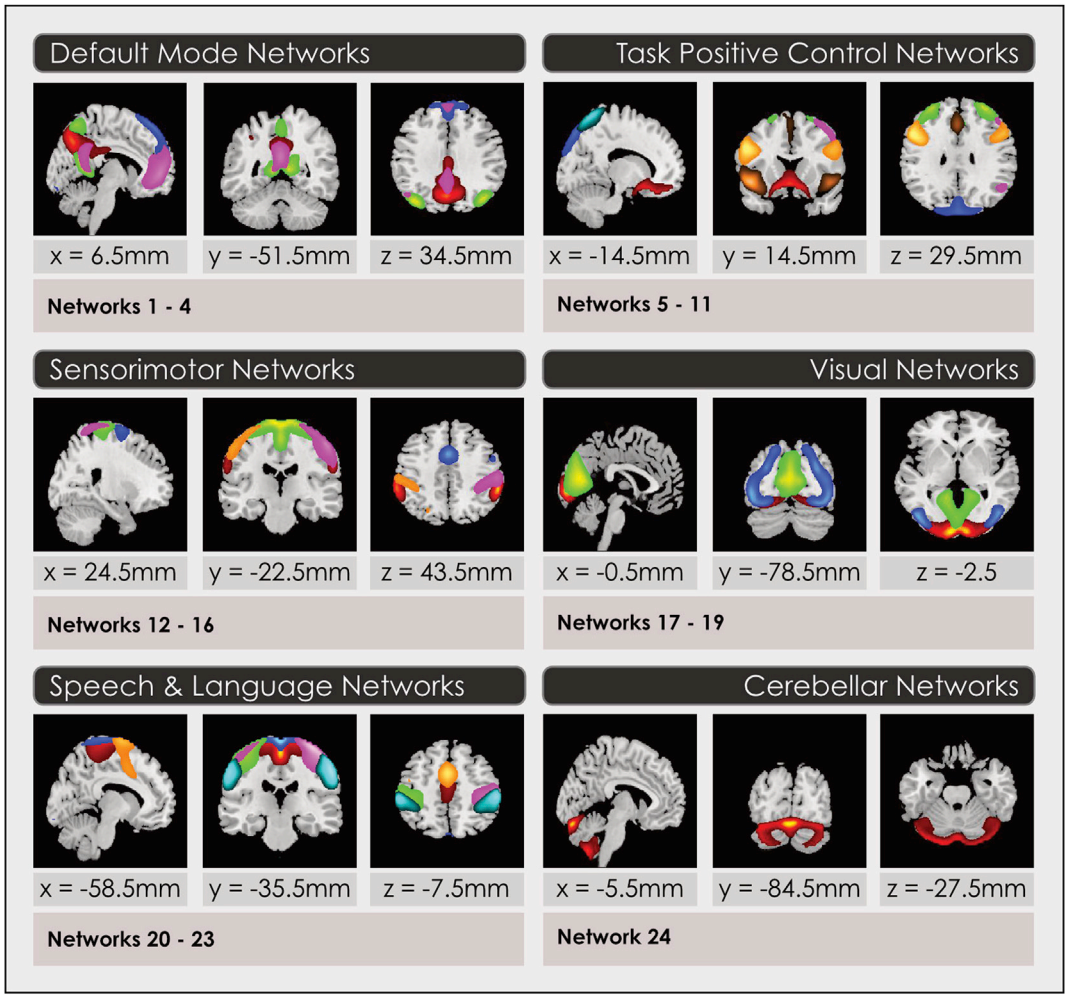

Fig. 2. Intrinsic networks grouped by neurocognitive function for the 24-network model. Group spatial maps are displayed in 2-dimensional format for a representative slice, for the 24-network model of intrinsic networks grouped by neurocognitive function. Spatial maps are created by thresholding gray-matter components from the group ICA at (mean + 4 standard deviations). Neurocognitive attributions were made using three methods described in the section **Functional Intrinsic Network Attribution and Grouping**. Readers may explore 3-dimensional maps of each network in Neurovault at https://neurovault.org/collections/4031/(24-network model) and https://neurovault.org/collections/4032/(51-network model), where networks are labelled with numbers and neurocognitive attributions.

2.5. Static functional connectivity analysis

We performed a multivariate analysis of covariance (MANCOVA) using the MANCOVAN toolbox and an established method (Allen et al., 2011) in GIFT, to compare the effects of sex with other possible predictors of variance in the 2 sets of network maps for the 534-subject motion-matched sample. To optimize for the large dimensions of the data but enable statistical testing at each voxel, predictors were submitted to the MANCOVA with an F-test at each iteration to produce a final reduced model for each outcome measure and network, before univariate testing of significant predictors was performed on the original model corrected for multiple comparisons (among all networks analyzed within a set) and false discovery rate (FDR) at $q = 0.01$. Nuisance regressors composed of individual scanner sites and the 6 realignment parameters and their 6 first derivatives were regressed from the analysis using the general linear model, prior to computing Pearson correlations between IN spatial maps. Each site was modeled as an individual regressor. We used age, gender, scan site and DVARS measure as predictors for all three analyses. Prior to computing sex-related effects on FNC matrices, we regressed the effects of age, IQ, scanner site and motion using the general linear model. While we did remove these effects, we nonetheless retained these as predictors in the MANCOVA to test for any residual effects of motion, age, IQ or site on results obtained in the statistical testing. For example, we tested for sex × DVARs interactions. Significant effects were computed for both male > female and female > male effects.

2.6. Dynamic connectivity analysis

2.6.1. Computation of brain states in native state space

To identify dynamic brain states, we adopted the framework (Allen et al., 2014; Sakoglu et al., 2010) of deriving small number of stable FNC states from fMRI ICA timecourses by applying a clustering algorithm to a succession of FNC windows. First, subject timecourses were detrended and despiked to remove outliers using 3dDespike in the AFNI software and filtered using a fifth-order Butterworth low-pass filter with a high frequency cutoff of 0.15 Hz. After regression of the 6 realignment parameters and their first temporal derivatives and scanner site from the timecourses, windowed covariance matrices were assembled using a sliding window approach instantiated in the temporal dFNC toolbox in GIFT where a tapered rectangular window was created by convolving a rectangle with a Gaussian and slid in steps of 1 TR. Windowed FNC covariance matrices (wFNC) were estimated using a graphical LASSO method (Friedman et al., 2008) as detailed in Allen et al. (2014). The window size was selected based on previous studies demonstrating window sizes in the range of 40–60s produce reasonable and robust results (Allen et al., 2014; Damaraju et al., 2014; de Lacy et al., 2017). We selected a window size = 17 TR for our baseline case and also performed sensitivity analyses at size = 15 TR and size = 20 TR. The k-means algorithm with city distance function was applied to the wFNC to derive stable dynamic states, initializing the clustering of data from all subjects with cluster centroids. These were first clustered using a subset of windows with local maxima in FC variance as in Allen et al. followed by clustering of the entire set of windows after initialization with the previous cluster solution (Allen et al., 2014). The subsampling procedure was performed to improve performance and reduce computational demand; previous results show that the solution improves results (Allen et al., 2014). We computed the number of clusters in the 24-network and 51-network models using the elbow criterion and the Bayes Information Criterion (BIC), testing over a range of 0–10 possible clusters. The elbow criterion indicated a cluster number of 4 in both the 24- and 51-network models for all window sizes (15, 17 and 20 TR). The BIC indicated 4 clusters for window size = 17 TR in both models, 5 clusters for window size = 20 TR in both models and 7 clusters in the 15TR/24-network model and 6 clusters in the 15 window/51-network model. Accordingly, a 4 cluster dFNC model with window size = 17 TR was selected as the baseline case for both 24-network and 51-network models with sensitivity analyses performed using other permutations suggested by the results obtained using the BIC, as well as a sensitivity analysis using absolute displacement in millimeters as the measurement of head motion instead of DVARS. Cluster membership as a function of time provides the state transition vector, indicating the state membership at a given point in time for each subject. In addition, we applied a threshold concept requiring that a given FNC covariance matrix be present in a minimum number of 10 windows for each subject included.

2.6.2. Measures of dynamism in native state space

We computed four measures of functional dynamism in the native state space i.e. on the stable brain states computed with k-means. These included three measures of fluidity: the number of times each subject moved between states during their individual timecourses (state-switching), the average time in windows they spent in each of the states once entering that state (dwell time), and the fraction of their total time spent in each state (fraction of time). We also computed FNC between pairwise INs within each state.

2.6.3. Computation of prototype connectivity patterns in meta-state space

To create prototype connectivity patterns (CPs) used in higher-dimensional measures of dynamism we followed a similar method but in this case preferred the use of the tICA algorithm (R. L. Miller et al., 2016). After creating wFNC series as detailed above, the tICA algorithm was applied to the individual arrays of FNC covariance matrices using the city method and the algorithm iterated a maximum of 200 times before convergence. We chose the tICA algorithm since its decomposition produces CPs whose weights in the wFNC are maximally temporally independent, leveraging higher order statistics. We have previously demonstrated that results using our dynamic measures (below) provided consistent results if other clustering measures such as k-means, spatial ICA and principal component analysis are used (R. L. Miller et al., 2016). CPs formed the analytic substrate for the remainder of the study.

2.6.4. High-dimension measures of dynamism in meta-state space

We computed four measures of dynamism in the higher-dimensional meta-state space using the same procedure as detailed in Miller et al. (R. L. Miller et al., 2014; R. L. Miller et al., 2016). Here, the time-varying, additive contributions made by CPs to each observed wFNC over the subject timecourses are discretized. A 4-dimensional weight vector is obtained representing the contribution of each CP to each wFNC matrix by regressing the FNC estimate onto the tICA cluster centroid. Real-valued weights accruing from this computation are then replaced by a value in ± (1, 2, 3, 4) according to the signed quartile into which each weight falls. The resulting discretized vectors are termed meta-states. Four measures of dynamism were computed for these meta-states. Discretization of the CP contributions to wFNC constructs a state space comprised of $8^4 = 4096$ possible meta-states (and similarly, 8^5, $8^6$and 8^7 possible states in the sensitivity analysis) which subjects may occupy over time. Two metrics describe the fluidity with which subjects traverse the meta-state space: the number of distinct meta-states passed through by each individual and the number of times each subject switches between meta-states. The remaining two metrics describe the high-dimension dynamic range achieved by subjects: the maximal L^1 span achieved between occupied meta-states, and the total distance 'traveled' by an individual through the state space (sum of all L^1 distances).

2.6.5. Dynamic statistical analysis

Sex-related differences in each measure of dynamic connectivity between males and females were calculated using two sample t-tests. These were computed at a significance level of $q < 0.05$, corrected to control FDR and multiple comparisons where relevant. Variance associated with site, DVARS measure, age and IQ-level was removed by regression using

the general linear model from the correlation values prior to performing clustering, in order that any sex-related effects would be examined in isolation. After removing the variance attributable to site, DVARS measure, age and IQ-level, we computed Pearson correlations between individual scores in the 5 secondary metrics of dynamism (state-switching in the native state space, and the meta-state measures) and individual scores in the Eriksen flanker task and task of mental rotation. For each correlation, we computed the correlation or r value and the significance or q value, correcting the latter for multiple comparisons by controlling for the false discovery rate (FDR) using the Benjamini-Hochberg procedure. Original study acronyms for each of the metrics obtained in individual testing in the flanker and mental rotation tasks may be viewed in Supplementary Table 3, which is a key prepared by the Brain Genomics Superstruct project team. We also computed sex-related performance differences in the two cognitive tasks using a *t*-test at a significance level of $p < 0.05$.

3. Results

3.1. Stronger static inter-network connections exist in males except among default mode sub-networks where connections were stronger in females

We first examined significant ($q < 0.01$, corrected for FDR and multiple comparisons) sex-related differences in the strength of static (averaged) connections among intrinsic networks. In general, we observed that static inter-network connections were stronger in males among networks in the task-positive control, sensorimotor, visual, language and subcortical groups (Fig. 3). We identified multiple sub-networks of the default mode system in our high-order models and connections among these sub-networks were stronger in females. This pattern was replicated in both the 24- and 51-network models.

Scattered exceptions existed. In particular, in a language network associated with semantic function (IN22, 24-network model) and in the orbito-frontal cortex and basal ganglia (IN10 and 49, 51-network model). There were no residual interactions between site, DVARS measure, age and IQ-level and the sex-related effects reported. For example, there were no sex × age interactions.

3.2. Sex-related differences in dynamic network connections vary significantly across transient brain states

Overall, the general pattern observed in static FNC was preserved in the dynamic analysis (Fig. 4). However, application of the time-windowing analytic technique exposed considerable variation in significant ($q < 0.05$, corrected for FDR and multiple comparisons) sex-related connectivity differences among the 4 brain states. More sex-related differences were observed in states 2–4. These states shared an overall pattern of stronger connections within individual network systems (grouped by neurocognitive associations) and anti-correlation with unrelated systems. This may be seen by observing the greater visual contrast between network groups on the diagonals of the matrices versus other cells in Figs. 4 and 5. By contrast, State 1 exhibited a divergent pattern of stronger connectivity more diffusely, and no sex-related differences were observed in this state. This general pattern was replicated in the 51-network model (Fig. 5).

We performed sensitivity analyses varying the number of windows to TR = 15 and TR = 20 for both the 24- and 51-network models using the 4-state construct which may be compared with our baseline parameter of TR = 17 in Supplementary Fig. 1. Similarly, sensitivity analyses related to the differential cluster numbers obtained in the BIC analysis were also performed. For the 24-network model, we show the results of a 7 cluster model with window size = 15 TR and 5 cluster model with window size = 20 TR in Supplementary Fig. 2. For the 51-network model we display the results of a 6 cluster model with window size = 15 TR and 5 cluster model with window size = 20 TR in Supplementary Fig. 3. Finally, the results of our sensitivity analysis using absolute displacement instead of DVARS may be viewed in Supplementary Fig. 4. In all cases, the main results were similar to those obtained in the baseline model seen in Figs. 4 and 5.

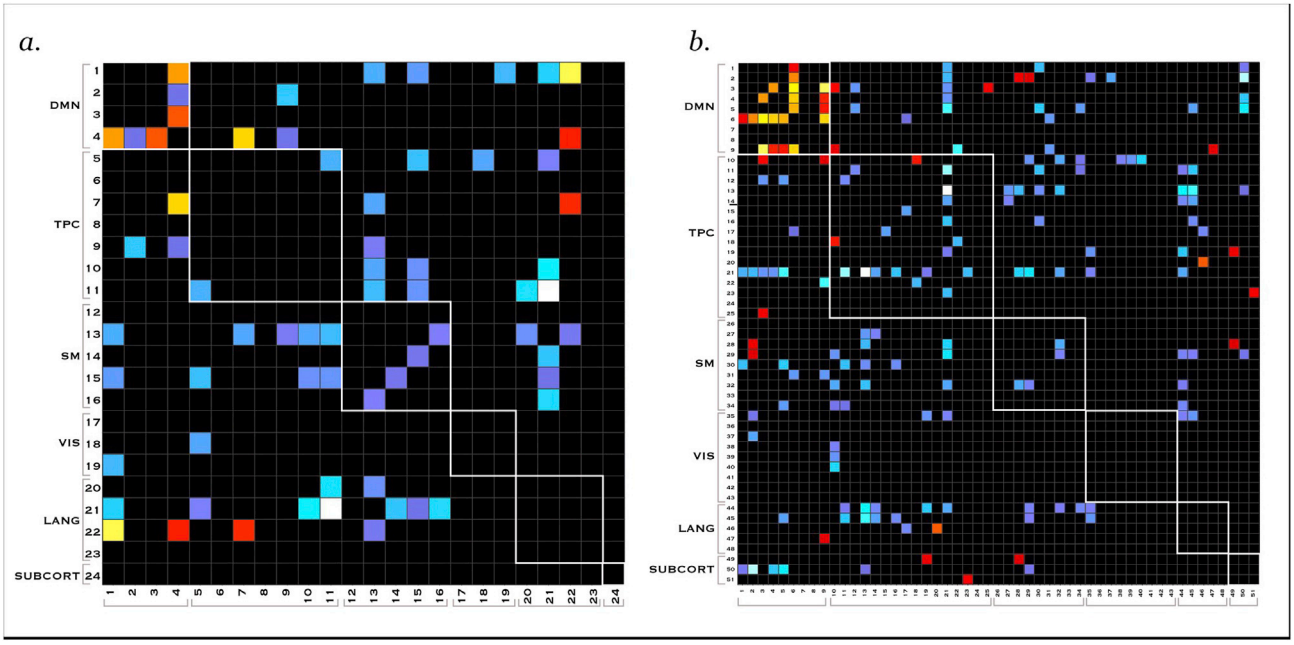

Fig. 3. Sex-related differences in static functional network connectivity in young adults. Sex-related effects in static connectivity in 534 typically-developing young adults matched for age, sex and head motion are displayed. Effects were determined by computing Pearson pairwise correlations averaged across fMRI timecourses for intrinsic networks obtained from ICA. In **a**, significant ($q < 0.01$ corrected for FDR and multiple comparisons) sex-related effects are displayed for the 24-network model, where **b** shows significant ($q < 0.01$ corrected for FDR and multiple comparisons) sex-related effects for the 51-network model. Effects are color-coded for female – male computations, where higher than average correlation strength (red, yellow) indicates higher connectivity in females, and lower than average correlation strength (blue) indicates higher connectivity in males.

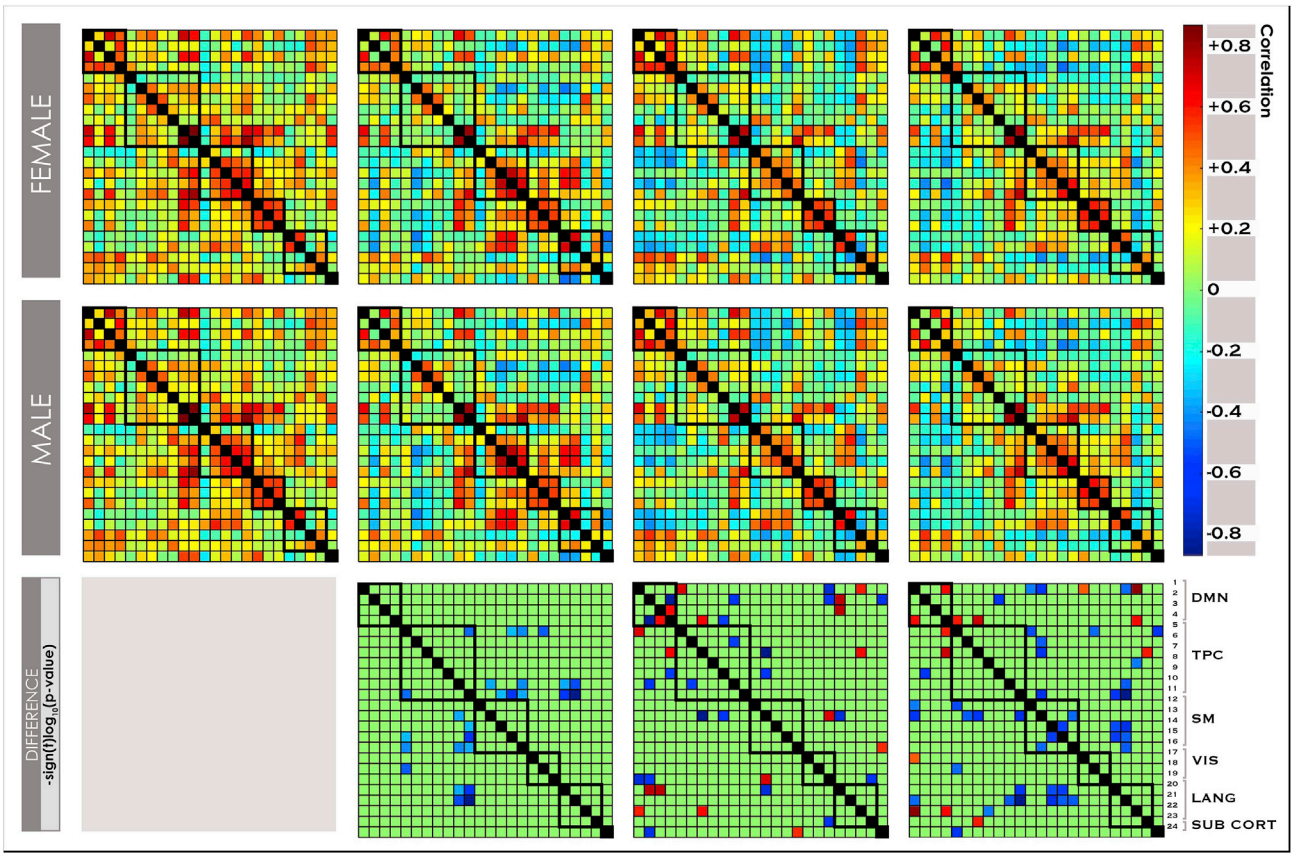

Fig. 4. Sex-related differences in dynamic functional connectivity in a 24-network model. Dynamic functional connectivity across 4 brain states was estimated with k-means clustering of windowed FNC matrices from 24 networks using ICA timecourses for females (top) and males (middle). Significant sex-related differences in FNC between all networks were computed for each of the 4 states using with 2-sample t-tests at a significance level of $q < 0.05$, corrected for false discovery rate and multiple comparisons.

3.3. Dynamic sex-related connectivity differences occur most frequently in brain states where neurocognitive systems display mutual anti-correlation

Our 51-network model provided increased resolution of sub-networks, allowing connectivity differences to be parsed in more detail. As remarked above, we identified a generalized pattern where sex-related differences in dynamic functional connectivity were more common in brain states with a higher connectivity 'gradient' between intra-system connections versus connections with non-member networks.

Of particular interest are the similarities and differences between states 3 and 4, where most sex-related differences occur. Both are characterized by well-defined connection strength within network systems and lack the strong anticorrelation between subcortical and other network systems seen in state 2. In state 3, diffuse anti-correlation exists between most network systems and non-member networks outside the 'home' system, and intra-DMN connectivity is robust. We identified the highest number of sex-related dynamic functional connectivity differences in this state. Significantly ($q < 0.05$, corrected for FDR and multiple comparisons) stronger connectivity in females than males in the DMN system and between the orbitofrontal network (IN10) and DMN networks was a prominent feature that differentiated this state. Elsewhere, significantly stronger connectivity was found in males than females, particularly between networks in the DMN and task-positive control systems and several other networks: the dorsolateral prefrontal cortex (IN22), a sensory-related insula network (IN21) and two sensorimotor networks (INs 30 and 31).

In state 4 we observed greater anti-correlation between the DMN and other network systems than in state 3. As well, we found relatively higher intra-system connectivity among visual and sensorimotor network groups, and stronger correlations between these groups and the task-positive control networks than in state 3. Females exhibited significantly ($q < 0.05$, corrected for FDR and multiple comparisons) stronger connectivity than males within the DMN system in this state, but this pattern was not as elaborated as in state 3. Males showed stronger connectivity than females in other network pairings, particularly between the supplementary motor cortex (IN31) and networks in the DMN and task-positive control systems. As reported in **3.3**, sensitivity analyses in the 51-network model may be viewed in Supplementary Figures 2, 3 and 4 and are concordant with these results.

3.4. Females spend significantly more time than males in a brain state where anticorrelation between network systems was maximized

We computed two measures related to the timing of transitions by subjects between the 4 brain states identified in this data: subjects' dwell time in each state and the fraction of time spent in each state. We observed significant ($q < 0.05$, corrected for FDR and number of comparisons) sex-related differences in dwell time in state 3, where females spent more time than males. This finding was replicated in both the 24-network and 51-network models (Fig. 6). Interestingly, a finding of females spending less time in state 2 than males also replicated in both models, but narrowly missed significance at $q = 0.066$ (24-network model) and $q = 0.087$ (51-network model), corrected for FDR.

An additional finding was that males spent a significantly ($q < 0.05$, corrected for FDR and number of comparisons) larger fraction of their total time in state 2 than females in the 51-network model (Table 2), but this did not replicate in the 24-network model ($q = 0.694$, corrected). These findings were replicated in the sensitivity analyses for both models.

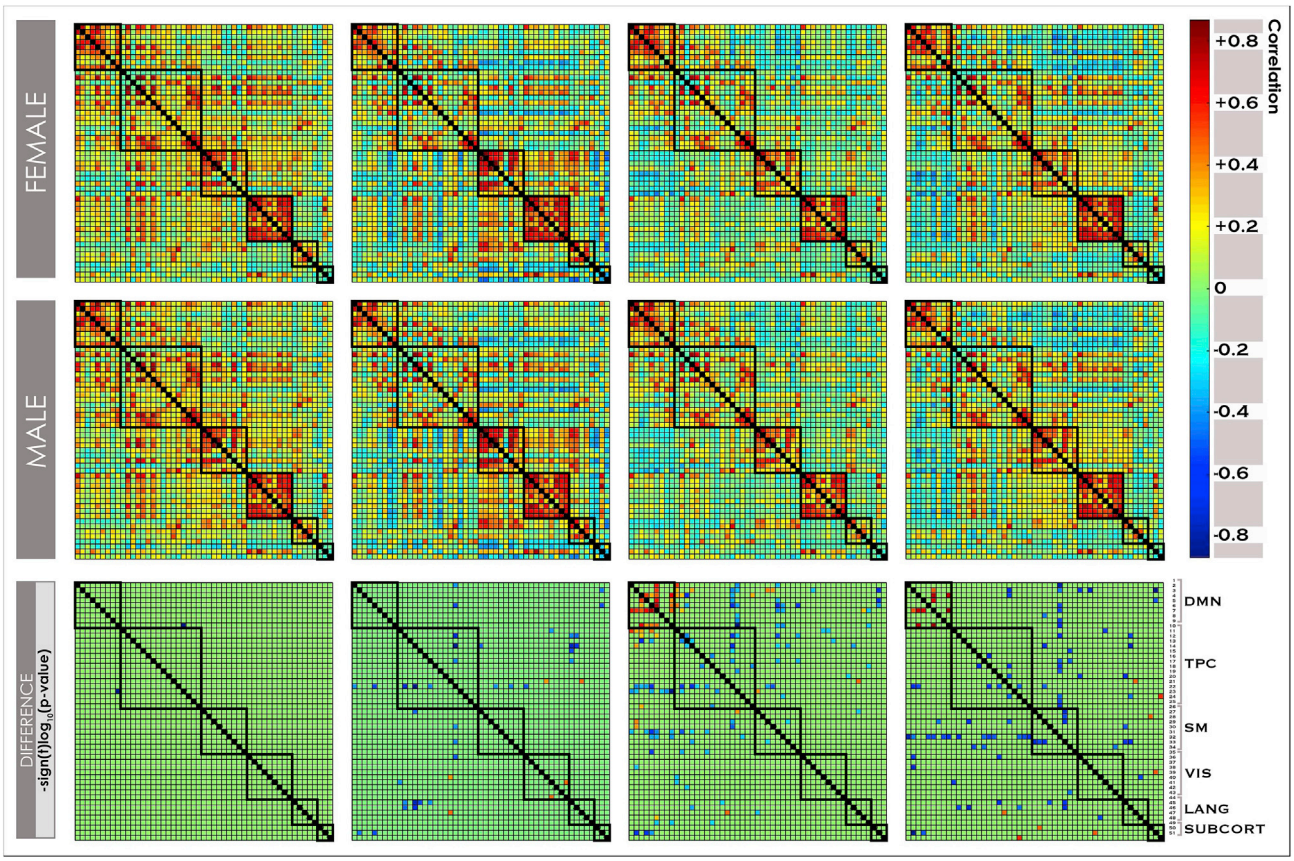

Fig. 5. Sex-related differences in dynamic functional connectivity in a 51-network model. Dynamic functional connectivity across 4 brain states was estimated with k-means clustering of windowed FNC matrices from 51 networks using ICA timecourses for females (top) and males (middle). Significant sex-related differences in FNC between all networks were computed for each of the 4 states using with 2-sample t-tests at a significant level of $q < 0.05$, corrected for false discovery rate and multiple comparisons.

3.5. Males exhibit greater brain functional dynamism than females

Five measures of dynamic fluidity and range across the native (state switching) and meta-state (number of states occupied, state-switching, L1 span, total L1 distance) subspaces were computed to delineate brain dynamism across the 24- and 51-network models. We identified statistically significant (p- or $q < 0.05$, corrected for FDR) sex-related differences in 4/10 of these measures of dynamism (Table 2). In every case, males exhibited significantly greater dynamism than females.

State-switching in the native state was significantly greater in males than females, replicated in all models. In the 24-network model, L1 span was significantly greater in males, replicating in all sensitivity analyses except the 15 TR/6-cluster model. Total L1 distance significantly greater than females in the 51-network model, a finding only replicated in the 15TR/6 cluster sensitivity analysis.

3.6. Brain functional dynamism is typically anti-correlated with response inhibition performance and positively correlated with mental rotation ability

In this sample, females performed significantly ($p < 0.05$) more slowly than males on 6/12 measures of response inhibition in the flanker task, and males performed better on 6/15 measures in a mental rotation task (Table 1, Supplementary Table 2). We quantified the relationship between task performance and dynamism by computing Pearson correlations between individual scores on the neurocognitive tasks and brain dynamism measures. The latter were typically - though not exclusively - anti-correlated with response inhibition and positively correlated with mental rotation ability.

3.6.1. Sex-related differences in response inhibition reaction times are significantly anti-correlated to multiple measures of brain dynamism particularly in females

In the response inhibition (Flanker) task, there were significant ($p < 0.05$) sex-related performance differences on all 6 measures of reaction time for correct responses (overall and during switch- and non-switch blocks) but no significant performance differences in measures of response correctness. Females had significantly longer reaction times than males (Table 1, Supplementary Table 2). In the combined sample, we observed significant ($q < 0.05$ corrected for FDR and multiple comparisons) correlations between multiple measures of reaction time performance and number of meta states and meta state-switching in the 24-network model and all four meta-state measures in the 51-network model (Fig. 7).

When females were considered separately in the 24-network model, there was a significant (corrected) correlation between native space state-switching and overall and switch-block correctness scores, and between meta-state number of states and many measures of both correctness and reaction time (Fig. 7a). In the 51-network model, females exhibited significant (corrected) correlations between most meta-state measures and measures of reaction time. The exception to the latter was an observed significant (corrected) correlation between native state-switching and overall percentage of correct responses (Fig. 7b). When males were considered separately, there were fewer significant ($q < 0.05$, corrected) correlations. These were present between both meta-state and native state-switching measures and reaction time performance during switch blocks in the 24-network model (Fig. 7a). In the 51-network model, significant (corrected) correlations were observed for males

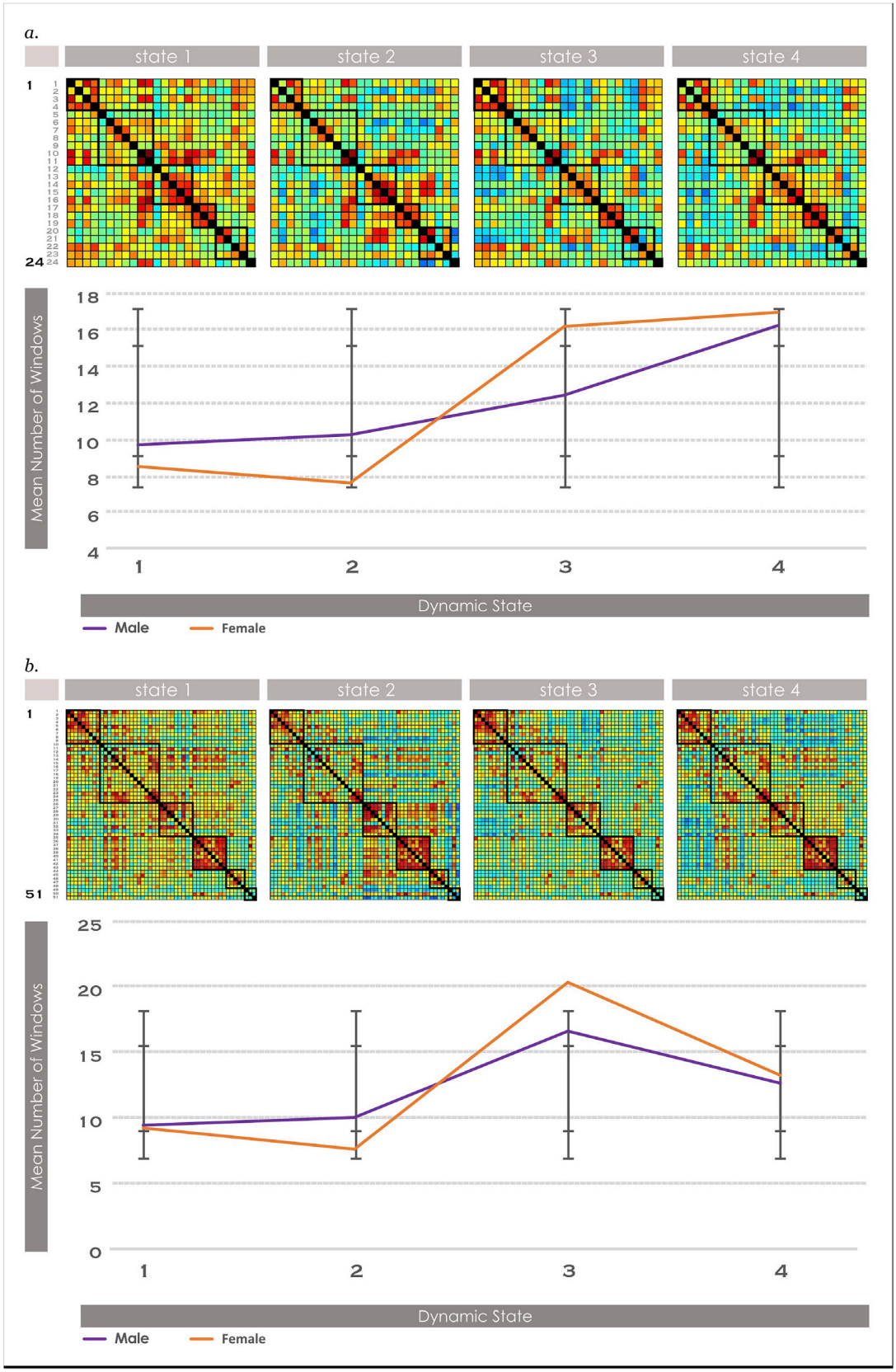

Fig. 6. Sex-related differences in dwell time in dynamic brain states. Dynamic functional connectivity across 4 brain states was estimated with k-means clustering of windowed FNC from the ICA timecourses for **a**, the 24-network model and **b**, the 51-network model. The dwell time within each state was computed for each subject. Significant FNC differences between networks in each model, and significant differences in dwell time, between females and males were examined with 2-sample t-tests at a significant level of $q < 0.05$, corrected for false discovery rate and multiple comparisons. Error bars are displayed for each curve showing the standard deviation.

Table 2
Sex-related differences in dynamic fluidity and range measures.

	Native Space			Meta-State Space			
	Dwell Time	Fraction of Time	State-switching	Number of states	State-switching	L1 Span	Total L1 Distance
24-Network Model	0.004-0.579	0.554-0.852	0.031	0.110	0.100	0.013	0.093
51-Network Model	0.037-0.971	0.004-0.602	0.005	0.127	0.144	0.211	0.046

Statistical significance level (p-value or q-value) is displayed for sex-related differences for dwell time, fraction of time and dynamism in 24- and 51-network models across 4 brain states from 2-sample t-tests performed at $p < 0.05$ or $q < 0.05$, corrected for FDR where appropriate. Statistically significant findings where females > males are highlighted in orange, and for males > females in blue. These values represent results after variance attributable to age, IQ and head motion statistics was removed using the general linear model. Dwell time and fraction of time values are shown in a range, indicating the lowest and highest bounds for each of the 5 states. In these measures, only the lowest values in the range, which are displayed in the table, achieved statistical significance.

between most meta-state measures and median switch block reaction times and meta-state number of states and total distance and mean switch block reaction times (Fig. 7b).

In the combined sample and males only, all significant relationships between measures of dynamism and response inhibition were directionally anti-correlated in both 24- and 51-network models. In females considered separately, we observed more significant correlations between measures of dynamism and response inhibition than in the combined or male samples in both models. In the four meta-state measures these were again consistently anti-correlated, in both 24- and 51-network models. Interestingly, in the native space state-switching measure alone, significant correlative relationships were positive. A full summary of results including task performance differences for each Flanker measure and correlation r and q values with each measure of dynamism may be accessed in Supplementary Table 2.

3.6.2. Sex-related differences in mental rotation performance are significantly positively correlated to multiple measures of brain dynamism, particularly in females

In mental rotation, we detected less consistent results between the 24- and 51-network models compared with the flanker task. In the 24-network model we observed significant ($q<0.05$, corrected) correlations between native space state-switching and 80-degree response times, and multiple meta-state measures and the percent of correct responses in 0-degree trials when females were considered separately. In the 0-degree mental rotation measure, males had significantly better performance than females (Table 1). There were no other significant results in the 24-network model. More observations were obtained in the 51-network model. In the whole sample including males and females, meta-state number of states was significantly ($q < 0.05$, corrected) correlated with 3 mental rotation measures of correct responses where males achieved significantly ($p < 0.05$) performance than females: 0- and 160-degree and total correct. State-switching in the native space was associated with the latter two of these (Fig. 8b). In females, many more measures of mental rotation performance were correlated with dynamism (Fig. 8b). Five measures (0-degree, median 80- and 120-degree, total and median total correct) were significantly ($q < 0.05$, corrected) correlated with both meta-state number of states and state switching. In addition, meta-state total distance was significantly ($q < 0.05$, corrected) correlated with 0-degree correct performance and native space state-switching with median 120-degree correct performance. In females these significant results were observed across measures with and without significant sex-related performance differences. In males considered separately, native space state-switching was again significantly ($q < 0.05$, corrected) correlated with 160-degree and total correct responses (Fig. 8b).

All significant ($q < 0.05$, corrected) correlations between mental rotation performance and measures of dynamism were detected in pairings between variables that exhibited positive correlation, directionally opposite to our findings in the flanker task. A full summary of results including task performance differences for each mental rotation measure and correlation r and q values with each measure of dynamism may be accessed in Supplementary Table 2.

4. Discussion

In recent years the analysis of dynamic, or time-varying, connectivity has attracted considerable attention (Preti et al., 2017). Windowing techniques can estimate transient brain states from fMRI data, and have proven their ability to detect differences attributed to the presence of neuropsychiatric diagnoses with observable sex/gender bias such as autism (de Lacy et al., 2017), bipolar disorder and schizophrenia (Rashid et al., 2014) and multiple sclerosis (Leonardi et al., 2013) as well as differential levels of consciousness (Amico et al., 2017). Functional brain dynamism has also been related to executive function ability and cognitive control. However, the degree to which males and females exhibit variance in their patterns of spatial dFNC and secondary metrics of brain dynamism was largely unknown. We performed an analysis of dFNC and dynamism in a large group of sex-, age- and motion-matched neurotypical young adults. Notwithstanding the considerable evidence that sex-related differences exist in certain neurocognitive tasks such as mental rotation, the question of whether sex-related differences exist in intrinsic brain function has been a thorny and ongoing debate. Our study provides the first evidence that significant sex-related differences exist in both dynamic connectivity among brain networks, and in certain secondary measures of macroscale brain dynamism, and that these may exhibit a directional relationship with cognitive abilities that also display sex-related differences in performance.

Initially, we performed a conventional survey of static, or time-averaged, FNC and found many significant differences in brain function between males and females. These organized around a theme of stronger connectivity in females than males within sub-networks of the default mode system and – typically - stronger connections in males than females in other network pairings. This result accords with prior studies that have positively identified significant sex-related differences in intrinsic brain functional connectivity. For example, Biswal et al. and Zuo et al. both identified sex-related differences in fronto-parietal, cingulo-opercular and temporal connections in typically-developing adults (Biswal et al., 2010; Zuo et al., 2010). Our results contrast with others who did not identify functional dimorphism. In particular, a prominent finding in our study was that connectivity among multiple sub-networks of the default mode system were stronger in females than males, replicated in both 24- and 51-network models. This differs from a study using rsfMRI performed

a.

	Flanker task measure											
	Flank_S_CORRpc	Flank_S_meanRTcorr	Flank_S_medRTcorr	Flank_S_score	Flank_NS_CORRpc	Flank_NS_meanRTcorr	Flank_NS_medRTcorr	Flank_NS_score	Flank_CORRpc	Flank_meanRTcorr	Flank_medRTcorr	Flank_TOT_score
BOTH SEXES												
Native space state-switching	-	-	-	-	-	-	-	-	-	-	-	-
Meta-state number of states	-	0.008	0.029	-	-	0.031	-	-	-	0.014	0.010	-
Meta-state state switching	-	0.003	0.012	-	-	-	-	-	-	0.006	0.025	-
Meta-State L1 span	-	-	-	-	-	-	-	-	-	-	-	-
Meta-state total distance	-	-	-	-	-	-	-	-	-	-	-	-
MALES ONLY												
Native space state-switching	-	0.021	0.040	-	-	-	-	-	-	-	-	-
Meta-state number of states	-	0.035	-	-	-	-	-	-	-	-	-	-
Meta-state state switching	-	0.020	0.034	-	-	-	-	-	-	-	-	-
Meta-State L1 span	-	-	-	-	-	-	-	-	-	-	-	-
Meta-state total distance	-	-	-	-	-	-	-	-	-	-	-	-
FEMALES ONLY												
Native space state-switching	0.049	-	-	0.049	-	-	-	-	0.030	-	-	0.038
Meta-state number of states	-	0.005	0.029	-	0.035	0.016	0.010	-	0.028	0.005	0.004	0.029
Meta-state state switching	-	0.012	-	-	-	0.039	0.024	0.030	0.045	0.014	0.010	0.030
Meta-State L1 span	-	-	-	-	-	-	-	-	-	-	-	-
Meta-state total distance	-	-	-	-	0.037	-	-	0.033	0.036	-	-	0.024

b.

	Flanker task measure											
	Flank_S_CORRpc	Flank_S_meanRTcorr	Flank_S_medRTcorr	Flank_S_score	Flank_NS_CORRpc	Flank_NS_meanRTcorr	Flank_NS_medRTcorr	Flank_NS_score	Flank_CORRpc	Flank_meanRTcorr	Flank_medRTcorr	Flank_TOT_score
BOTH SEXES												
Native space state-switching	-	-	-	-	-	-	-	-	-	-	-	-
Meta-state number of states	-	0.003	-	-	-	0.017	0.017	-	-	0.004	0.008	-
Meta-state state switching	-	0.029	0.003	-	-	0.033	0.023	-	-	0.005	0.003	-
Meta-State L1 span	-	0.002	0.003	-	-	-	-	-	-	0.028	-	-
Meta-state total distance	-	0.002	0.002	-	-	0.014	0.038	-	-	0.003	0.003	-
MALES ONLY												
Native space state-switching	-	-	-	-	-	-	-	-	-	-	-	-
Meta-state number of states	-	0.040	0.030	-	-	-	-	-	-	-	-	-
Meta-state state switching	-	-	-	-	-	-	-	-	-	-	-	-
Meta-State L1 span	-	-	0.033	-	-	-	-	-	-	-	-	-
Meta-state total distance	-	0.015	0.008	-	-	-	-	-	-	0.027	0.037	-
FEMALES ONLY												
Native space state-switching	0.005	-	-	-	-	-	-	-	-	-	-	-
Meta-state number of states	-	0.030	-	-	-	0.016	0.011	-	-	0.022	-	-
Meta-state state switching	-	0.001	0.004	-	-	0.013	0.004	-	-	0.002	0.001	-
Meta-State L1 span	-	0.001	0.002	-	-	0.004	0.002	-	-	0.001	0.001	-
Meta-state total distance	-	0.003	0.007	-	-	-	-	-	-	0.004	0.002	-

Fig. 7. Significant relationships between brain dynamism and response inhibition. Statistical significance level (q-value) is displayed for significant ($q < 0.05$) correlations between each measure of functional brain dynamism and measures of response inhibition (Flanker task) in ***a.*** 24-network and ***b.*** 51-network models of brain function. All values represent significant Pearson correlations corrected for FDR. Empty cells indicate insignificant results ($q > 0.05$).

a.

Mental rotation task measure

	MenRot_0_CORRpc	MenRot_0_meanRTcorr	MenRot_0_medRTcorr	MenRot_80_CORRpc	MenRot_80_meanRTcorr	MenRot_80_medRTcorr	MenRot_120_CORRpc	MenRot_120_meanRTcorr	MenRot_120_medRTcorr	MenRot_160_CORRpc	MenRot_160_meanRTcorr	MenRot_160_medRTcorr	MenRot_TOT_CORRpc	MenRot_TOT_meanRTcorr	MenRot_TOT_medRTcorr
BOTH SEXES															
Native space state-switching	-	-	-	-	-	-	-	-	-	-	-	-	-	-	-
Meta-state number of states	-	-	-	-	-	-	-	-	-	-	-	-	-	-	-
Meta-state state switching	-	-	-	-	-	-	-	-	-	-	-	-	-	-	-
Meta-State L1 span	-	-	-	-	-	-	-	-	-	-	-	-	-	-	-
Meta-state total distance	-	-	-	-	-	-	-	-	-	-	-	-	-	-	-
MALES ONLY	-	-	-	-	-	-	-	-	-	-	-	-	-	-	-
Native space state-switching	-	-	-	-	-	-	-	-	-	-	-	-	-	-	-
Meta-state number of states	-	-	-	-	-	-	-	-	-	-	-	-	-	-	-
Meta-state state switching	-	-	-	-	-	-	-	-	-	-	-	-	-	-	-
Meta-State L1 span	-	-	-	-	-	-	-	-	-	-	-	-	-	-	-
Meta-state total distance	-	-	-	-	-	-	-	-	-	-	-	-	-	-	-
FEMALES ONLY															
Native space state-switching	-	-	-	-	0.038	0.006	-	-	-	-	-	-	-	-	-
Meta-state number of states	0.011	-	-	-	-	-	-	-	-	-	-	-	-	-	-
Meta-state state switching	0.004	-	-	-	-	-	-	-	-	-	-	-	-	-	-
Meta-State L1 span	-	-	-	-	-	-	-	-	-	-	-	-	-	-	-
Meta-state total distance	0.032	-	-	-	-	-	-	-	-	-	-	-	-	-	-

b.

Mental rotation task measure

	MenRot_0_CORRpc	MenRot_0_meanRTcorr	MenRot_0_medRTcorr	MenRot_80_CORRpc	MenRot_80_meanRTcorr	MenRot_80_medRTcorr	MenRot_120_CORRpc	MenRot_120_meanRTcorr	MenRot_120_medRTcorr	MenRot_160_CORRpc	MenRot_160_meanRTcorr	MenRot_160_medRTcorr	MenRot_TOT_CORRpc	MenRot_TOT_meanRTcorr	MenRot_TOT_medRTcorr
BOTH SEXES															
Native space state-switching	-	-	-	-	-	-	-	-	-	0.016	-	-	0.022	-	-
Meta-state number of states	0.047	-	-	-	-	-	-	-	-	0.044	-	-	0.039	-	-
Meta-state state switching	-	-	-	-	-	-	-	-	-	-	-	-	-	-	-
Meta-State L1 span	-	-	-	-	-	-	-	-	-	-	-	-	-	-	-
Meta-state total distance	-	-	-	-	-	-	-	-	-	-	-	-	0.049	-	-
MALES ONLY															
Native space state-switching	-	-	-	-	-	-	-	-	-	0.000	-	-	0.002	-	-
Meta-state number of states	-	-	-	-	-	-	-	-	-	-	-	-	-	-	-
Meta-state state switching	-	-	-	-	-	-	-	-	-	-	-	-	-	-	-
Meta-State L1 span	-	-	-	-	-	-	-	-	-	-	-	-	-	-	-
Meta-state total distance	-	-	-	-	-	-	-	-	-	-	-	-	-	-	-
FEMALES ONLY															
Native space state-switching	-	-	-	-	-	-	-	-	0.008	-	-	-	-	-	-
Meta-state number of states	0.002	-	-	-	-	0.023	-	-	0.005	-	-	-	0.011	-	0.011
Meta-state state switching	0.002	-	-	-	0.028	0.031	-	-	0.046	0.008	-	-	0.042	-	0.018
Meta-State L1 span	-	-	-	-	-	-	-	-	-	-	-	-	-	-	-
Meta-state total distance	0.012	-	-	-	-	-	-	-	-	-	-	-	-	-	-

Fig. 8. Significant relationships between brain dynamism and mental rotation. Statistical significance level (q-value) is displayed for significant ($q < 0.05$) correlations between each measure of functional brain dynamism and measures of performance on a mental rotation task in ***a.*** 24-network and ***b.*** 51-network models of brain function. All values represent significant Pearson correlations corrected for FDR. Empty cells indicate insignificant results ($q > 0.05$).

by Weissman-Fogel et al. (2010) which examined connectivity within a single identified default mode network in a smaller sample of right-handed young adults ($n = 49$), which did not identify sex-related differences in the functional connections within the network. Differences with our results might be due to methodology, since this group used a different ICA-based technique, and did not match subjects for age or head motion, or covary for or remove the variance associated with variables such as age, motion or IQ. In our study, subjects were matched for age, sex and head motion, and the variance associated with age, head motion, IQ and scanner site were regressed from network correlations prior to performing statistical analysis. However, our findings accord closely with earlier work by Allen et al. which controlled for, but did not remove, variance associated with age. This single-scanner study examined sFNC in 28 intrinsic networks in 603 neurotypical adults from a different sample population, and identified significant dimorphism in the connections among many networks. This study also detected stronger connectivity among subnetworks of the default mode system in females, and typically stronger sFNC among other networks in males: the same

pattern that we identified (See Fig. 8 in (Allen et al., 2011)).

We identified significant sex-related differences in most but not all dynamic connectivity states. While sharing the overall theme identified in the static connectivity benchmark analysis, the estimation of separable dynamic brain states allowed us to demonstrate that sex-related differences manifest transiently over the timecourse of functional imaging. We found that no differences in inter-network connectivity manifested between males and females in one dynamic state, while in others sex-related differences were prolific. These latter instances occurred in states characterized by greater anti-correlation among network neurocognitive systems. For example, between networks in the default mode system and other network types. State 3, with the most marked anti-correlated pattern, also proved to be the state where the largest number of connectivity differences occurred, and was also the only state where significant, replicable differences in a timing measure were identified. Females spent significantly more time than males in this state. This apparent 'sensitivity' to the manifestation of sex-related connectivity and timing differences in states with greater anti-correlation may relate to the extensive body of work characterizing relationships between default mode and task-positive networks. In the established model, a fundamental anti-correlation between the functional operations of default mode ('interiorly-focused) and task-positive ('exteriorly-focused) intrinsic control networks is posited in the resting state, first identified by Fox et al. (2005) and validated in other studies. In turn, this model may ultimately relate to tentative models of brain functional control during task performance, where task-positive fronto-parietal and cingulo-opercular networks are proposed to control the initiation and maintenance of task-positive states versus switching into 'task-negative' activation of default mode networks. Our study suggests that further investigation of potential sex-related differences in task switching is warranted to ascertain if males and females perform state-switching operations differently. More specifically, future work may test the hypothesis of whether functional anti-correlation relates to stronger intra-default mode connections in females and an increased ability to remain in the anti-correlated state while males preserve stronger inter-network connections among other task-positive systems.

Of note, the larger theme we observed of stronger connections between default mode sub-networks in females contrasting with otherwise stronger connectivity in males was broadly shared between the sFNC and dFNC analysis. This is consistent with prior work suggesting the connectivity patterns identifiable in static analysis represent a superordinate approximation of underlying dynamic brain 'states' (Ciric et al., 2017). A degree of commonality is to be expected, where dFNC teases out increased detail that is approximated in the sFNC analysis. Bifurcation between female vs male patterns of dynamic connectivity strength and functional dynamism may link to other broad themes in the neuroimaging literature. While this must be speculative, it is intriguing to theorize the possible implications of stronger female intrinsic functional connectivity – both static and dynamic – within the default mode system. Given its established links to mentalizing, introspection and social cognition, this observation may help explain parallel findings of superior female performance in these types of neurocognitive tasks and bears further investigation. In addition, this sex-related difference in default mode functional connectivity may prove a moderating influence in neurocognitive disorders such as autism and ADHD, which have a marked male > female bias in incidence, and which have both been well-linked to disrupted default mode function. For example, our own recent work in youth with ADHD identified a subnetwork of the default mode system that displayed a significant sex × diagnosis interaction (de Lacy et al., 2018), and similar results have been obtained in the default mode system in autism (J. Yang and Lee, 2018).

Besides measures of connectivity and timing, we also analyzed sex-related differences in measures of brain functional dynamism. In these metrics, we characterize relative male and female dynamism over the native state space and over subspaces derived from prototype connectivity states. These metrics quantify dynamic fluidity and range, with intuitive appeal as corollaries of cognitive control and flexibility. We found that males exhibited greater dynamism than females in several metrics. In particular, our finding of increased state-switching in males > females replicated in both network models, indicating greater fluidity of movement among dynamic states obtained using spatial dFNC. In comparison Yaesoubi et al. used the tICA algorithm to define 5 maximally temporally independent states in a 50-network model in 405 subjects (200 female) and examined gender differences in occupancy patterns of these states, and combinations of states. The degree of age and motion-matching was not specified. After regressing out age, they found that males experienced a significantly larger number of distinct state combinations than females (Yaesoubi et al., 2015). While this is not a directly analogous measure to those we surveyed, it does indicate a somewhat similar theme of greater dynamism in males. In our present analysis we removed the variance attributable to age in order to focus our experiments on sex-related differences in dFNC and measures of dynamism given the small extant evidence base, and did not explore interactions between age and sex. However, important functional connectivity changes occur during human development and our findings support the need for future studies examining the potential for age × sex interactions.

A small body of existing work has explored the relationship between neurocognitive abilities and brain dynamics. For the most part, this has focused on cognitive control and executive function. Yang et al. examined dwell time in 5 dynamic states preferentially associated with various subregions of the posteromedial cortex, and demonstrated a relationship between the dynamic properties of a visual subregion and individual performance in a measure of concept formation and mental flexibility (Z. Yang et al., 2014). Using Human Connectome Project (HCP) data, Jia et al. used multi-level adaptive clustering within the sliding window framework to show that lower functional coupling transition time, or greater dynamism, had superior ability to predict variance in a range of tasks (alertness, cognition, emotion and personality traits) than static FNC analysis (Jia et al., 2014). Nomi et al. also used HCP data and employed a processing methodology similar in part to our own to examine relationships between dynamic timing measures and the Flanker task, Wisconsin Card Sort (cognitive flexibility), Penn Progressive Matrices (fluid intelligence) and tasks of processing speed and working memory, in a 100-network, 5-state model with gender as a nuisance variable. They found that cognitive flexibility and processing speed displayed weak positive and negative correlations with the fraction of time spent in various brain states (Nomi et al., 2017). While these analyses did not focus specifically on relationships between neurocognitive performance and higher-level brain dynamics as we do in the present study, collectively they suggest that dynamic connectivity properties can be linked to cognitive control abilities.

We found that females were significantly less apt to switch connectivity states and ranged over smaller state spaces (L1 span and distance), while displaying generally slower reaction times in the Eriksen flanker task. In the latter test of response inhibition and cognitive control, we identified a negative correlation between task response times and multiple meta-state measures of dynamism, that was more common in females. Our results detected a clear signal in the flanker task, segregating slower task performance (reaction time) with dynamism. Thus, our findings preliminarily suggest that meta-state measures of dynamism are negatively correlated with response inhibition, and that significantly lower dynamic fluidity and range in females may be associated with their slower rates of response inhibition. It might be hypothesized that the relatively greater dynamic 'stickiness' that females exhibit, with increased dwell time and reduced fluidity and range, contributes to their tendency to inhibit unwanted responses more slowly. In contrast, mental rotation is a visuospatial processing task in which males both in the present study and in the established literature have consistently demonstrated superior performance versus females. Mental rotation tasks typically demand that subjects visualize the rotation of objects in space before correctly matching them with exemplars, and is thought to

involve iterative testing (rotations) and comparisons before a decision is made as to a correct match. We are not aware of prior studies done to relate brain functional dynamics to mental rotation. Our results suggest that increased dynamism is positively correlated with mental rotation performance, perhaps generating the hypothesis that a subject with a greater dynamic 'search space' may perform better at the iterative problem-solving involved in this task. While the signal we detected in mental rotation was less clear than in the flanker, it did again suggest that the relationship between dynamism and task performance was stronger in females.

4.1. Limitations

Limitations exist in the present study. Firstly, IQ scores derived from the Shipley-Hartford Age-Corrected T-scores were provided in the original dataset and used in the current analysis. These are estimates of IQ rather than the result of full IQ testing. As may be seen in Table 1, the average estimated IQ of this sample is above the population average due to the recruitment method, and results may not be fully extensible to broader populations. Further, our study includes only young neurotypical individuals and results may vary in younger or older subjects and individuals with neuropsychiatric differences, particularly cognitive differences. We provide two models of whole brain function derived from spatial group ICA, with 24- and 51-network functional parcellations, and sensitivity analyses with window sizes of 15-, 17- and 20 TR as well as different cluster numbers and measures of head motion based on our prior work in parameterizing dynamic connectivity analysis. However, this is not an exhaustive set of possible parameters. For example, the number of ICA components could be further varied to higher or lower numbers. While our two models were in broad agreement, different results might be obtained if other analytic choices were made. Finally, given the resting state condition, it is possible that subject vigilance or wakefulness may have been reduced during part or all of their scans, or varied among subjects and this may have affected results.

5. Conclusion

Taken together, our results demonstrate that sexual dimorphism is present in human brain dynamic connectivity and in multiple high-order measures of brain dynamism, as well as validating prior work that sex-related differences exist in static intrinsic connectivity. We also provide the first evidence suggesting a link between differential neurocognitive performance by males and females and brain functional dynamics. Our results build on prior evidence that brain functional dynamism may provide biological correlates that help explain neurocognitive performance and abilities and that these may include sex-related differences. Reduced dynamism in females, who spend more time in certain brain states and switch states less frequently, may provide a 'stickier' functional substrate associated with their slower reaction times in the flanker task of cognitive inhibition, whereas males exhibit greater dynamic fluidity, change between certain states more often and range over a larger state space, achieving superior performance in certain elements of mental rotation, which demands an iterative visualization and problem-solving approach. Future research that examines sex-related differences in dynamism in a wider range of tasks, and includes imaging obtained during task performance, will inform the hypotheses generated by this study. We acknowledge that the identification of significant sex-related differences in brain function does not imply a causal relationship with sex-related differences in cognition or behavior, or vice versa, since function-behavior relationships are complex in humans. Importantly, our analysis establishes correlations rather than causality, and no conclusions can be drawn as to the cause of the observed sex-related connectivity differences in this study sample. The development of functional brain connectivity continues during maturation and into young adulthood (Power et al., 2010) and many biological, behavioral and environmental factors are known to impact brain function and likely influence differences between groups, including sex-related differences. There is considerable individual variation and sex-related differences may exist on a spectrum. However, the findings of this and other studies support the need for further investigation of the influence of sex-related differences in functional connectivity, dynamic connectivity and brain function more broadly (Fine, 2014), and how these develop into adulthood. We conclude that sex is an important variable to consider in fMRI experiments and the analysis of brain function and hope that our findings will stimulate further study of sex-related differences in dynamic connectivity and its potential relationship to spheres of human cognition.

Conflicts of interest

The authors declare no conflicts of interest.

Acknowledgements

The authors gratefully acknowledge the help of B. Ernesto Johnson in preparing figures. This study was supported by the National Center for Advancing Translational Sciences of the National Institutes of Health under Award Number KL2TR000421 to NdL, and NIH 2R01EB005846, P20GM103472, P30GM122734 and R01EB020407 and NSF 153906 to VDC. The content is solely the responsibility of the authors and does not necessarily represent the official views of the NIH. NL designed the study, performed the analysis and wrote the paper. VC helped design the study and contributed to writing the paper. NK and EM contributed to study design and writing the paper.

Data were provided in part by the Brain Genomics Superstruct Project of Harvard University and the Massachusetts General Hospital, (Principal Investigators: Randy Buckner, Joshua Roffman, and Jordan Smoller), with support from the Center for Brain Science Neuroinformatics Research Group, the Athinoula A. Martinos Center for Biomedical Imaging, and the Center for Human Genetic Research. 20 individual investigators at Harvard and MGH generously contributed data to the overall project.

Appendix A. Supplementary data

Supplementary data to this article can be found online at https://doi.org/10.1016/j.neuroimage.2019.116116.

References

Allen, E.A., Damaraju, E., Plis, S.M., Erhardt, E.B., Eichele, T., Calhoun, V.D., 2014. Tracking whole-brain connectivity dynamics in the resting state. Cerebr. Cortex 24 (3), 663–676. https://doi.org/10.1093/cercor/bhs352.

Allen, E.A., Erhardt, E.B., Damaraju, E., Gruner, W., Segall, J.M., Silva, R.F., Calhoun, V.D., 2011. A baseline for the multivariate comparison of resting-state networks. Front. Syst. Neurosci. 5, 2. https://doi.org/10.3389/fnsys.2011.00002.

Allen, E.A., Erhardt, E.B., Wei, Y., Eichele, T., Calhoun, V.D., 2012. Capturing inter-subject variability with group independent component analysis of fMRI data: a simulation study. Neuroimage 59 (4), 4141–4159. https://doi.org/10.1016/j.neuroimage.2011.10.010.

Amico, E., Marinazzo, D., Di Perri, C., Heine, L., Annen, J., Martial, C., Goni, J., 2017. Mapping the functional connectome traits of levels of consciousness. Neuroimage 148, 201–211. https://doi.org/10.1016/j.neuroimage.2017.01.020.

Biswal, B.B., Mennes, M., Zuo, X.N., Gohel, S., Kelly, C., Smith, S.M., Milham, M.P., 2010. Toward discovery science of human brain function. Proc. Natl. Acad. Sci. U. S. A. 107 (10), 4734–4739. https://doi.org/10.1073/pnas.0911855107.

Calhoun, V.D., Adali, T., 2012. Multisubject independent component analysis of fMRI: a decade of intrinsic networks, default mode, and neurodiagnostic discovery. IEEE Rev. Biomed. Eng. 5, 60–73. https://doi.org/10.1109/RBME.2012.2211076.

Calhoun, V.D., Adali, T., Pearlson, G.D., Pekar, J.J., 2001. A method for making group inferences from functional MRI data using independent component analysis. Hum. Brain Mapp. 14 (3), 140–151.

Calhoun, V.D., Miller, R., Pearlson, G., Adali, T., 2014. The chronnectome: time-varying connectivity networks as the next frontier in fMRI data discovery. Neuron 84 (2), 262–274. https://doi.org/10.1016/j.neuron.2014.10.015.

Christodoulou, A.G., Bauer, T.E., Kiehl, K.A., Feldstein Ewing, S.W., Bryan, A.D., Calhoun, V.D., 2013. A quality control method for detecting and suppressing uncorrected residual motion in fMRI studies. Magn. Reson. Imaging 31 (5), 707–717. https://doi.org/10.1016/j.mri.2012.11.007.

Ciric, R., Nomi, J.S., Uddin, L.Q., Satpute, A.B., 2017. Contextual connectivity: a framework for understanding the intrinsic dynamic architecture of large-scale functional brain networks. Sci. Rep. 7 (1), 6537. https://doi.org/10.1038/s41598-017-06866-w.

Damaraju, E., Allen, E.A., Belger, A., Ford, J.M., McEwen, S., Mathalon, D.H., Calhoun, V.D., 2014. Dynamic functional connectivity analysis reveals transient states of dysconnectivity in schizophrenia. Neuroimage Clin. 5, 298–308. https://doi.org/10.1016/j.nicl.2014.07.003.

De Bellis, M.D., Keshavan, M.S., Beers, S.R., Hall, J., Frustaci, K., Masalehdan, A., Boring, A.M., 2001. Sex differences in brain maturation during childhood and adolescence. Cerebr. Cortex 11 (6), 552–557.

de Lacy, N., Doherty, D., King, B.H., Rachakonda, S., Calhoun, V.D., 2017. Disruption to control network function correlates with altered dynamic connectivity in the wider autism spectrum. Neuroimage Clin. 15, 513–524. https://doi.org/10.1016/j.nicl.2017.05.024.

de Lacy, N., Kodish, I., Rachakonda, S., Calhoun, V.D., 2018. Novel in silico multivariate mapping of intrinsic and anticorrelated connectivity to neurocognitive functional maps supports the maturational hypothesis of ADHD. Hum. Brain Mapp. https://doi.org/10.1002/hbm.24187.

Dosenbach, N.U., Fair, D.A., Miezin, F.M., Cohen, A.L., Wenger, K.K., Dosenbach, R.A., Petersen, S.E., 2007. Distinct brain networks for adaptive and stable task control in humans. Proc. Natl. Acad. Sci. U. S. A. 104 (26), 11073–11078. https://doi.org/10.1073/pnas.0704320104.

Dosenbach, N.U., Visscher, K.M., Palmer, E.D., Miezin, F.M., Wenger, K.K., Kang, H.C., Petersen, S.E., 2006. A core system for the implementation of task sets. Neuron 50 (5), 799–812. https://doi.org/10.1016/j.neuron.2006.04.031.

Du, Y., Allen, E.A., He, H., Sui, J., Wu, L., Calhoun, V.D., 2016. Artifact removal in the context of group ICA: a comparison of single-subject and group approaches. Hum. Brain Mapp. 37 (3), 1005–1025. https://doi.org/10.1002/hbm.23086.

Erhardt, E.B., Rachakonda, S., Bedrick, E.J., Allen, E.A., Adali, T., Calhoun, V.D., 2011. Comparison of multi-subject ICA methods for analysis of fMRI data. Hum. Brain Mapp. 32 (12), 2075–2095. https://doi.org/10.1002/hbm.21170.

Fine, C., 2014. Neuroscience. His brain, her brain? Science 346 (6212), 915–916. https://doi.org/10.1126/science.1262061.

Fox, M.D., Snyder, A.Z., Vincent, J.L., Corbetta, M., Van Essen, D.C., Raichle, M.E., 2005. The human brain is intrinsically organized into dynamic, anticorrelated functional networks. Proc. Natl. Acad. Sci. U. S. A. 102 (27), 9673–9678. https://doi.org/10.1073/pnas.0504136102.

Friedman, J., Hastie, T., Tibshirani, R., 2008. Sparse inverse covariance estimation with the graphical lasso. Biostatistics 9 (3), 432–441. https://doi.org/10.1093/biostatistics/kxm045.

Guadalupe, T., Mathias, S.R., vanErp, T.G.M., Whelan, C.D., Zwiers, M.P., Abe, Y., Francks, C., 2017. Human subcortical brain asymmetries in 15,847 people worldwide reveal effects of age and sex. Brain Imag. Behav. 11 (5), 1497–1514. https://doi.org/10.1007/s11682-016-9629-z.

Gur, R.C., Alsop, D., Glahn, D., Petty, R., Swanson, C.L., Maldjian, J.A., Gur, R.E., 2000. An fMRI study of sex differences in regional activation to a verbal and a spatial task. Brain Lang. 74 (2), 157–170. https://doi.org/10.1006/brln.2000.2325.

Himberg, J., Hyvarinen, A., Esposito, F., 2004. Validating the independent components of neuroimaging time series via clustering and visualization. Neuroimage 22 (3), 1214–1222. https://doi.org/10.1016/j.neuroimage.2004.03.027.

Holmes, A.J., Hollinshead, M.O., O'Keefe, T.M., Petrov, V.I., Fariello, G.R., Wald, L.L., Buckner, R.L., 2015. Brain Genomics Superstruct Project initial data release with structural, functional, and behavioral measures. Sci. Data 2, 150031. https://doi.org/10.1038/sdata.2015.31.

Hutchison, R.M., Womelsdorf, T., Allen, E.A., Bandettini, P.A., Calhoun, V.D., Corbetta, M., Chang, C., 2013. Dynamic functional connectivity: promise, issues, and interpretations. Neuroimage 80, 360–378. https://doi.org/10.1016/j.neuroimage.2013.05.079.

Im, K., Lee, J.M., Lee, J., Shin, Y.W., Kim, I.Y., Kwon, J.S., Kim, S.I., 2006. Gender difference analysis of cortical thickness in healthy young adults with surface-based methods. Neuroimage 31 (1), 31–38. https://doi.org/10.1016/j.neuroimage.2005.11.042.

Ingalhalikar, M., Smith, A., Parker, D., Satterthwaite, T.D., Elliott, M.A., Ruparel, K., Verma, R., 2014a. Reply to Joel and Tarrasch: on misreading and shooting the messenger. Proc. Natl. Acad. Sci. U. S. A. 111 (6), E638.

Ingalhalikar, M., Smith, A., Parker, D., Satterthwaite, T.D., Elliott, M.A., Ruparel, K., Verma, R., 2014b. Sex differences in the structural connectome of the human brain. Proc. Natl. Acad. Sci. U. S. A. 111 (2), 823–828. https://doi.org/10.1073/pnas.1316909110.

Jamadar, S.D., Sforazzini, F., Raniga, P., Ferris, N.J., Paton, B., Bailey, M.J., Group, A.I., 2018. Sexual dimorphism of resting-state network connectivity in healthy ageing. J. Gerontol. B Psychol. Sci. Soc. Sci. https://doi.org/10.1093/geronb/gby004.

Jia, H., Hu, X., Deshpande, G., 2014. Behavioral relevance of the dynamics of the functional brain connectome. Brain Connect. 4 (9), 741–759. https://doi.org/10.1089/brain.2014.0300.

Joel, D., Tarrasch, R., 2014. On the mis-presentation and misinterpretation of gender-related data: the case of Ingalhalikar's human connectome study. Proc. Natl. Acad. Sci. U. S. A. 111 (6), E637. https://doi.org/10.1073/pnas.1323319111.

Laird, A.R., Fox, P.M., Eickhoff, S.B., Turner, J.A., Ray, K.L., McKay, D.R., Fox, P.T., 2011. Behavioral interpretations of intrinsic connectivity networks. J. Cogn. Neurosci. 23 (12), 4022–4037. https://doi.org/10.1162/jocn_a_00077.

Lenroot, R.K., Giedd, J.N., 2008. The changing impact of genes and environment on brain development during childhood and adolescence: initial findings from a neuroimaging study of pediatric twins. Dev. Psychopathol. 20 (4), 1161–1175. https://doi.org/10.1017/S0954579408000552.

Lenroot, R.K., Gogtay, N., Greenstein, D.K., Wells, E.M., Wallace, G.L., Clasen, L.S., Giedd, J.N., 2007. Sexual dimorphism of brain developmental trajectories during childhood and adolescence. Neuroimage 36 (4), 1065–1073. https://doi.org/10.1016/j.neuroimage.2007.03.053.

Leonardi, N., Richiardi, J., Gschwind, M., Simioni, S., Annoni, J.M., Schluep, M., Van De Ville, D., 2013. Principal components of functional connectivity: a new approach to study dynamic brain connectivity during rest. Neuroimage 83, 937–950. https://doi.org/10.1016/j.neuroimage.2013.07.019.

Li, Y.O., Adali, T., Calhoun, V.D., 2007. Estimating the number of independent components for functional magnetic resonance imaging data. Hum. Brain Mapp. 28 (11), 1251–1266. https://doi.org/10.1002/hbm.20359.

McCarthy, M.M., 2016. Multifaceted origins of sex differences in the brain. Philos. Trans. R. Soc. Lond. B Biol. Sci. 371 (1688), 20150106. https://doi.org/10.1098/rstb.2015.0106.

Miller, D.I., Halpern, D.F., 2014. The new science of cognitive sex differences. Trends Cogn. Sci. 18 (1), 37–45. https://doi.org/10.1016/j.tics.2013.10.011.

Miller, R.L., Yaesoubi, M., Calhoun, V.D., 2014. Higher dimensional analysis shows reduced dynamism of time-varying network connectivity in schizophrenia patients. Conf. Proc. IEEE Eng. Med. Biol. Soc. 2014, 3837–3840. https://doi.org/10.1109/EMBC.2014.6944460.

Miller, R.L., Yaesoubi, M., Turner, J.A., Mathalon, D., Preda, A., Pearlson, G., Calhoun, V.D., 2016. Higher dimensional meta-state analysis reveals reduced resting fMRI connectivity dynamism in schizophrenia patients. PLoS One 11 (3), e0149849. https://doi.org/10.1371/journal.pone.0149849.

Mutlu, A.K., Schneider, M., Debbane, M., Badoud, D., Eliez, S., Schaer, M., 2013. Sex differences in thickness, and folding developments throughout the cortex. Neuroimage 82, 200–207. https://doi.org/10.1016/j.neuroimage.2013.05.076.

Nomi, J.S., Vij, S.G., Dajani, D.R., Steimke, R., Damaraju, E., Rachakonda, S., Uddin, L.Q., 2017. Chronnectomic patterns and neural flexibility underlie executive function. Neuroimage 147, 861–871. https://doi.org/10.1016/j.neuroimage.2016.10.026.

Power, J.D., Fair, D.A., Schlaggar, B.L., Petersen, S.E., 2010. The development of human functional brain networks. Neuron 67 (5), 735–748. https://doi.org/10.1016/j.neuron.2010.08.017.

Power, J.D., Mitra, A., Laumann, T.O., Snyder, A.Z., Schlaggar, B.L., Petersen, S.E., 2014. Methods to detect, characterize, and remove motion artifact in resting state fMRI. Neuroimage 84, 320–341. https://doi.org/10.1016/j.neuroimage.2013.08.048.

Preti, M.G., Bolton, T.A., Van De Ville, D., 2017. The dynamic functional connectome: state-of-the-art and perspectives. Neuroimage 160, 41–54. https://doi.org/10.1016/j.neuroimage.2016.12.061.

Rashid, B., Damaraju, E., Pearlson, G.D., Calhoun, V.D., 2014. Dynamic connectivity states estimated from resting fMRI Identify differences among Schizophrenia, bipolar disorder, and healthy control subjects. Front. Hum. Neurosci. 8, 897. https://doi.org/10.3389/fnhum.2014.00897.

Raznahan, A., Lee, Y., Stidd, R., Long, R., Greenstein, D., Clasen, L., Giedd, J.N., 2010. Longitudinally mapping the influence of sex and androgen signaling on the dynamics of human cortical maturation in adolescence. Proc. Natl. Acad. Sci. U. S. A. 107 (39), 16988–16993. https://doi.org/10.1073/pnas.1006025107.

Sacher, J., Neumann, J., Okon-Singer, H., Gotowiec, S., Villringer, A., 2013. Sexual dimorphism in the human brain: evidence from neuroimaging. Magn. Reson. Imaging 31 (3), 366–375. https://doi.org/10.1016/j.mri.2012.06.007.

Sakoglu, U., Pearlson, G.D., Kiehl, K.A., Wang, Y.M., Michael, A.M., Calhoun, V.D., 2010. A method for evaluating dynamic functional network connectivity and task-modulation: application to schizophrenia. Magma 23 (5–6), 351–366. https://doi.org/10.1007/s10334-010-0197-8.

Satterthwaite, T.D., Wolf, D.H., Roalf, D.R., Ruparel, K., Erus, G., Vandekar, S., Gur, R.C., 2015. Linked sex differences in cognition and functional connectivity in youth. Cerebr. Cortex 25 (9), 2383–2394. https://doi.org/10.1093/cercor/bhu036.

Seeley, W.W., Menon, V., Schatzberg, A.F., Keller, J., Glover, G.H., Kenna, H., Greicius, M.D., 2007. Dissociable intrinsic connectivity networks for salience processing and executive control. J. Neurosci. 27 (9), 2349–2356. https://doi.org/10.1523/JNEUROSCI.5587-06.2007.

Smith, S.M., Fox, P.T., Miller, K.L., Glahn, D.C., Fox, P.M., Mackay, C.E., Beckmann, C.F., 2009. Correspondence of the brain's functional architecture during activation and rest. Proc. Natl. Acad. Sci. U. S. A. 106 (31), 13040–13045. https://doi.org/10.1073/pnas.0905267106.

Spreng, R.N., Sepulcre, J., Turner, G.R., Stevens, W.D., Schacter, D.L., 2013. Intrinsic architecture underlying the relations among the default, dorsal attention, and frontoparietal control networks of the human brain. J. Cogn. Neurosci. 25 (1), 74–86. https://doi.org/10.1162/jocn_a_00281.

Stoet, G., Geary, D.C., 2013. Sex differences in mathematics and reading achievement are inversely related: within- and across-nation assessment of 10 years of PISA data. PLoS One 8 (3), e57988. https://doi.org/10.1371/journal.pone.0057988.

Vernet, M., Quentin, R., Chanes, L., Mitsumasu, A., Valero-Cabre, A., 2014. Frontal eye field, where art thou? Anatomy, function, and non-invasive manipulation of frontal regions involved in eye movements and associated cognitive operations. Front. Integr. Neurosci. 8, 66. https://doi.org/10.3389/fnint.2014.00066.

Voyer, D., Voyer, S., Bryden, M.P., 1995. Magnitude of sex differences in spatial abilities: a meta-analysis and consideration of critical variables. Psychol. Bull. 117 (2), 250–270.

Weissman-Fogel, I., Moayedi, M., Taylor, K.S., Pope, G., Davis, K.D., 2010. Cognitive and default-mode resting state networks: do male and female brains "rest" differently? Hum. Brain Mapp. 31 (11), 1713–1726. https://doi.org/10.1002/hbm.20968.

Yaesoubi, M., Miller, R.L., Calhoun, V.D., 2015. Mutually temporally independent connectivity patterns: a new framework to study the dynamics of brain connectivity

at rest with application to explain group difference based on gender. Neuroimage 107, 85–94. https://doi.org/10.1016/j.neuroimage.2014.11.054.

Yang, J., Lee, J., 2018. Different aberrant mentalizing networks in males and females with autism spectrum disorders: evidence from resting-state functional magnetic resonance imaging. Autism 22 (2), 134–148. https://doi.org/10.1177/1362361316667056.

Yang, Z., Craddock, R.C., Margulies, D.S., Yan, C.G., Milham, M.P., 2014. Common intrinsic connectivity states among posteromedial cortex subdivisions: insights from analysis of temporal dynamics. Neuroimage 93 (Pt 1), 124–137. https://doi.org/10.1016/j.neuroimage.2014.02.014.

Yarkoni, T., Poldrack, R.A., Nichols, T.E., Van Essen, D.C., Wager, T.D., 2011. Large-scale automated synthesis of human functional neuroimaging data. Nat. Methods 8 (8), 665–670. https://doi.org/10.1038/nmeth.1635.

Zuo, X.N., Kelly, C., Di Martino, A., Mennes, M., Margulies, D.S., Bangaru, S., Milham, M.P., 2010. Growing together and growing apart: regional and sex differences in the lifespan developmental trajectories of functional homotopy. J. Neurosci. 30 (45), 15034–15043. https://doi.org/10.1523/JNEUROSCI.2612-10.2010.